Title

Fibre-specific mitochondrial protein abundance is linked to resting and post-training mitochondrial content in human muscle.

Author list

E. Reisman[1,2,12], J. Botella[1,3,12], C. Huang[4], R. B. Schittenhelm[4], D. A. Stroud[5,6,7], C. Granata[1,,8,9,10], S. Chandrasiri[1], G. Ramm[11], V. Oorschot[11,12], N. J. Caruana[1,5*] & D. J. Bishop[1*]

Affiliations

1. Institute for Health and Sport (iHeS), Victoria University, Melbourne, Victoria, 3011, Australia
2. Mary MacKillop Institute for Health Research, Australian Catholic University, Melbourne, Victoria, 3000, Australia
3. Metabolic Research Unit, School of Medicine and Institute for Mental and Physical Health and Clinical s Translation (IMPACT), Deakin University, Waurn Ponds, Victoria, 3216, Australia.
4. Monash Proteomics & Metabolomics Facility, Biomedicine Discovery Institute and Department of Biochemistry and Molecular Biology, Monash University, Clayton, Victoria, 3168, Australia
5. Department of Biochemistry and Pharmacology, Bio21 Molecular Science and Biotechnology Institute, The University of Melbourne, Parkville, Victoria, 3052, Australia
6. Murdoch Children's Research Institute, Royal Children's Hospital, Parkville, Victoria, 3052, Australia
7. Victorian Clinical Genetics Services, Royal Children's Hospital, Parkville, Victoria, 3052, Australia
8. Department of Diabetes, Central Clinical School, Monash University, Melbourne, Victoria, 3004, Australia
9. Institute for Clinical Diabetology, German, Diabetes Center, Leibniz Center for Diabetes Research at Heinrich-Heine-University, Düsseldorf, Düsseldorf, 40225, Germany
10. German Center for Diabetes Research, Partner Düsseldorf, München-Neuherberg, 40225, Germany
11. Ramaciotti Centre for Cryo EM, Biomedicine Discovery Institute and Department of Biochemistry and Molecular Biology, Monash University, Clayton, Victoria, 3168, Australia
12. Electron Microscopy Core Facility, European Molecular Biology Laboratory, Heidelberg, 69117, Germany

12. These authors contributed equally to this work

* Correspondence: David.Bishop@vu.edu.au, nikeisha.caruana@vu.edu.au

Abstract

Analyses of mitochondrial adaptations in human skeletal muscle have mostly used whole-muscle samples, where results may be confounded by the presence of a mixture of type I and II muscle fibres. Using our adapted mass spectrometry-based proteomics workflow, we provide new insights into fibre-specific mitochondrial differences in human skeletal muscle before and after training. Our findings challenge previous conclusions regarding the extent of fibre-type-specific remodelling of the mitochondrial proteome and highlight that most baseline differences in mitochondrial protein abundances between fibre types reported by us, and others, might be due to differences in total mitochondrial content or a consequence of adaptations to habitual physical activity (or inactivity). Most training-induced changes in different mitochondrial functional groups, in both fibre types, were stoichiometrically linked to changes in markers of mitochondrial content.

Keywords: Proteomics, single fibre, exercise, complex IV, fatty acid oxidation

Introduction

The remarkable ability of skeletal muscle to adapt to repeated contractile stimuli is one of the most fundamental and intriguing aspects of physiology [1]. Repeated exercise sessions (i.e., exercise training) alter the expression of proteins, which can lead to improved maintenance of cellular homeostasis [2], altered metabolism [3], and the prevention and treatment of many chronic diseases [4]. Exercise is also a potent stimulus to activate mitochondrial biogenesis [5, 6 7], with resulting increases in mitochondrial protein content and respiratory function [8, 9]. These adaptations appear to depend on the characteristics of the exercise stimulus [10, 11].

One limitation of most human training studies to date is the analysis of whole-muscle samples, where the results may be confounded by divergent changes in different fibre types [12]. Human skeletal muscle is composed of three major fibre types (type I, IIa, and IIx), which differ in their contractile, metabolic, and bioenergetic characteristics; this is reflected by a greater reliance on mitochondrial oxidative enzyme activity in type I fibres [13, 14, 15] and greater glycolytic enzyme activity in type II fibres [16]. Furthermore, Henneman's size principle [17] proposes that type I fibres have a lower threshold of activation, and will be recruited at lower exercise intensities, whereas fast-twitch fibres (type IIa and IIx) have a higher activation threshold and will be increasingly recruited at greater exercise intensities [18, 19]. Skeletal muscle fibre recruitment is therefore related to exercise intensity [18, 19], and it has been hypothesised that higher exercise intensities might stimulate greater adaptations in type II fibres relative to lower intensities [17, 20, 21]. It has also been proposed that recruitment of type II fibres may help to explain the greater mitochondrial adaptations reported following high-intensity training [11, 18, 19, 22]. Until recently, however, technical limitations have prevented the direct assessment of fibre-type-specific adaptations to different types of exercise training.

Modifications to immunoblotting protocols have enabled researchers to identify training-induced adaptations of mitochondrial proteins in single skeletal muscle fibres [23, 24, 25, 26]. However, due to limited starting material, only five of the more than 1100 known mitochondrial proteins have been investigated to date [12, 23, 24, 25, 26, 27]. Improvements in mass-spectrometry-based proteomic techniques have allowed greater resolution of the contractile and metabolic features of single skeletal muscle fibre types – first in mice [28] and then in humans [29]. The detection of functionally important, low-abundance proteins, in addition to thousands of other proteins, was a significant development that has advanced our understanding of the breadth and complexity of proteins at the fibre level in skeletal muscle. Recent work has built on this research and adapted this technique to investigate fibre-type-specific protein changes to moderate-intensity training in the skeletal muscle of a small

number of males (n=5) [30]. To date, however, no proteomic study has investigated the effects of divergent exercise intensities, which differ in their recruitment of the major fibre types, on fibre-type-specific mitochondrial adaptations. A greater understanding of fibre-type-specific adaptations to different exercise intensities may help to optimise the prescription of exercise to prevent and treat diseases, as well as counteract some of the detrimental effects of ageing.

In the present study, we developed a sensitive mass spectrometry-based (MS) proteomics workflow that allowed for the pooling of single muscle fibres, and the utilisation of tandem mass tag (TMT) labelling, to facilitate the identification of low abundant mitochondrial proteins. To investigate potential fibre-type-specific changes in protein abundances following exercise training, we employed two very different training interventions - moderate-intensity continuous training (MICT) and sprint-interval training (SIT). These two types of training were chosen as they differ in intensity (i.e., moderate versus very high intensity) and have been reported to require different skeletal muscle fibre recruitment patterns [22, 27, 31]. In contrast to the only published single-fibre proteomic study to examine the effects of exercise training [30], we did not detect any significant changes in the abundance of individual proteins in either fibre type following either training type. This finding, based on our more robust statistical approach, raises important questions regarding the ability of current single-fibre studies to avoid false positives and to confidently detect training-induced changes of individual proteins in single-fibre pools. While were able to detect fibre-specific changes in different mitochondrial functional groups following training, many of these differences were no longer apparent when corrected for training-induced changes in mitochondrial content. Thus, most training-induced changes in mitochondrial protein abundances were stoichiometrically linked to the overall increase in mitochondrial content. Despite the hypothesis that SIT would target type II fibres, we observed few differentially expressed protein functional groups following SIT. A novel finding was that there was a decreased abundance of complex IV subunits in both type I and II fibres following SIT.

RESULTS AND DISCUSSION

Single-fibre proteomics

Only two studies in young men, both with small sample sizes (n = 4 and 5, respectively), have employed proteomics to describe fibre-type-specific differences for the contractile and metabolic features of human skeletal muscle fibres [29, 30]. In the present study, we present the data from sixteen recreationally active, healthy men who completed one of two 8-week training interventions - either moderate-intensity continuous training (MICT; n = 8) or very high-intensity sprint-interval training

(SIT; n = 8) (see Table S1 – Tab 1 for participant characteristics). Before (PRE) and after training (POST), skeletal muscle biopsies were collected from the vastus lateralis muscle and single fibres were isolated, fibre-typed, pooled, and analysed utilising the proteomic workflow described in Figure 1a.

One of the challenges of analysing skeletal muscle is the large dynamic range of protein concentrations caused by the highly abundant sarcomeric proteins, which account for over 50% of the total protein content [28, 32, 33, 34], while proteins from all other muscle compartments, including the mitochondria, are confined to the lower half of the abundance range [34]. Compared to typical whole-tissue proteomic studies, single-muscle fibres provide very low protein yields [28, 35], which further complicates the identification of lower abundant proteins [34, 36]. While previous studies have used label-free quantitative shotgun approaches after filter-aided sample preparation [29, 30], we chose a workflow incorporating tandem mass tag (TMT) labelling, which not only allowed us to increase sample size and throughput to accommodate our complex experimental design investigating two different exercise intensities but also exhibits higher quantitative precision than label-free quantification [37, 38].

Our approach identified a total of 3141 proteins across all pooled samples, with 81% (2534 proteins) of these identified with high confidence (false discovery rate [FDR] < 0.05) and > 1 unique peptide (Table S1-Tab 2). On average, we were able to reliably identify 1849 ± 59 (1477 to 1999) high-confidence proteins per pooled single-fibre sample (Figures S2a, b, & c, Table S9 – Tab 1). Proteins were removed from our dataset, as well as as in comparative datasets from Deshmukh (2021) and Murgia (2017), if they contained more than 70% missing values, leaving a total dataset across all samples in our study of 1600 proteins (Table S1-Tab 3). This cut-off is designed to remove the bulk of missing data, which can cause further downstream bias, but still allow appropriate imputation of missing values for analysis.

To further understand the characteristics of the fibre-specific proteome, we examined the cellular localisation of the proteins identified in each individual sample of pooled type I or type II fibres based on Gene Ontology Cellular Components (GOCCs). GO enrichment analysis of our dataset (Figure 1b, Table S1-Tab 4) demonstrates good coverage of the structural and metabolic features of the muscle fibre proteome, including contractile, sarcomeric, ribosomal, and mitochondrial proteins.

To assess the comprehensiveness of our protein detection in pooled single fibres, we compared our dataset to the two previous studies [29, 30] investigating the single muscle fibre proteome in humans

(Figure 1c, Table S1-Tab 5). There were 844 proteins in common between the three studies, which may represent proteins that can more confidently be used to compare fibre types in human skeletal muscle. One of the most significantly enriched cellular components for these commonly identified proteins was the mitochondrion (Figure 1d, Table S1-Tab 6).

Fibre type differences in the pre-training samples

Multi-dimensional scaling revealed a good separation of the protein profiles between pooled type I and type II single fibre samples pre-training (Figure 1e). Proteomic features of the different fibre-type pools are presented in a volcano plot (Figure 1f). A total of 206 proteins were identified as differentially expressed between fibre types pre-training (PRE), using an empirical Bayes method and with statistical significance set at an adjusted P value cut-off of 0.05 (Table S1-Tab 7). Our results are similar to Deshmukh (2021) [30], which identified 232 differentially expressed proteins between fibre types (reanalysed by us with the same imputation and empirical Bayes methods as our study). Unsupervised hierarchical clustering revealed a clear separation of fibre types, although, as expected, there was some biological variability amongst individuals (Figure 1g).

Our analysis revealed new contractile proteins with fibre-type-specific expression profiles (Table S1-Tab 8). These included MYH3 and MYL4 – two poorly understood members of the myosin family [39]. We also observed many of the expected differences between fibre types. Type I fibres were characterised by a greater abundance of contractile proteins belonging to the myosin heavy (MYH7) and light (MYL6B) chains, as well as troponin (TNNT1, TNNC1, TNNI1) and an isoform of the sarcoplasmic reticulum Ca^{2+}-ATPase (ATP2A2, also named SERCA2; [40, 41]), while type II fibres possessed a greater abundance of MYH2, MYL1, TNNT3, TNNC2, TNNI2, and also ACTN3.

Most studies on muscle fibre heterogeneity have focused on contractile proteins [33, 42]. However, as confirmed in our study, the diversity between muscle fibres is not only restricted to contractile proteins but extends to a wide range of subcellular systems - including ionic transport, cellular calcium signalling, and metabolism [42]. Approximately 30% of the proteins identified as differentially expressed between fibre types were mitochondrial – with most of these mitochondrial proteins (~ 90%) having a greater abundance in type I fibres. These differentially expressed mitochondrial proteins were enriched in pathways associated with fatty acid oxidation, as well as other proteins involved in the electron transport chain (Table S1-Tab 7).

Influence of mitochondrial content on fibre-type-specific expression profiles

Of the 390 mitochondrial proteins quantified in the present study, 314 (~ 70%) were also quantified in the previous two single-fibre proteomic studies (Figure 2a, Table S2-Tab 1). The top 5 GO Biological Process (BP) terms for these commonly detected mitochondrial proteins were related to mitochondrial electron transport (NADH to ubiquinone and respiratory chain complex I assembly), the tricarboxylic acid cycle, fatty acid beta-oxidation, and mitochondrial ATP synthesis coupled proton transport (Figure 2b, Table S2-Tab 2). Many of these mitochondrial proteins had a significantly greater abundance in type I fibres (Figure 2c – top panel, Table S1-Tab 7), which is consistent with the superior capacity of type I fibres for mitochondrial oxidative phosphorylation and fatty acid oxidation [43].

An important question that has not been adequately addressed is whether these fibre-type-specific expression profiles for mitochondrial proteins are independent of the greater mitochondrial content in type I versus type II human skeletal muscle fibres [13, 44, 45]. To examine the potential influence of mitochondrial content on fibre-type-specific expression profiles observed for mitochondrial proteins, we first calculated the mitochondrial protein enrichment (MPE) – a value that identifies the contribution of mitochondrial protein intensities to the overall detectable proteome [8]. Consistent with previous research [30], there was a greater abundance of proteins associated with the mitochondria cellular component in type I compared to type II fibres (Figure 2d, Table S2-Tab 5). As this supported an overall greater content of mitochondria in type I versus type II fibres in our participants, we next employed our previously described mitochondrial normalisation strategy [8], which aims to correct for the bias introduced by differences in total mitochondrial content. This allowed us to compare the abundance of individual mitochondrial proteins relative to the mitochondrial proteome in each fibre type (i.e., mitochondria-corrected relative abundance).

Post normalisation, less than one-third of the mitochondrial proteins we had observed to have a greater abundance in type I fibre pools remained differentially expressed (compare Figure 2c – bottom panel, Table S2-Tab 7, with Figure 2c – top panel, Table S1-Tab 7). This analysis suggests that many of the differences in mitochondrial protein abundances between fibre types reported by us, and others [29, 30], might be due to differences in total mitochondrial content rather than fibre-type-specific remodelling of the mitochondrial proteome. With this approach, we also identified nine

additional mitochondrial proteins with a greater abundance in type II than type I fibres; these proteins included ALDH1B1, SDHA, RIDA, SLC25A12, GRSF1, PARK7, HSPE1, GPX4, PNPO (Figure 2c). None of these nine mitochondrial proteins had previously been reported to be differentially expressed in type II versus type I muscle fibres, and further research is required to explore their potential role in functional differences between the fibre types.

Proteomic responses to different types of training in type I and type II skeletal muscle fibres

Only one published proteomic study has examined fibre-type-specific adaptations to one type of exercise training (1 h at 75 to 90% of maximum heart rate, 4x/week for 12 weeks) in human skeletal muscle [30]. However, no study has investigated if there are fibre-type-specific changes to the proteome that depend on the nature of the exercise stimulus. The size principle states that type I fibres are mostly utilised at lower exercise intensities, whereas type II fibres are increasingly recruited at higher exercise intensities [17, 21]. Therefore, a long-standing hypothesis is that training-induced changes to the proteome in response to low-intensity exercise will mostly be confined to the type I fibres that are predominantly recruited with this type of exercise [19, 46]. In contrast, higher-intensity exercise (e.g., all-out sprinting) has been proposed to stimulate greater adaptations in type II fibres compared to exercise performed at lower intensities [47].

To investigate potential fibre-type-specific changes to the proteome in response to divergent exercise stimuli, we analysed the data from 16 healthy young men who trained 3 to 4 times per week for 8 weeks after random assignment to one of two very different types of training – MICT or SIT (Figure 3a). By design, both exercise groups had very different exercise prescription characteristics; there was a 4.7-fold greater exercise intensity for SIT and a 5.2-fold greater training volume for MICT (Figure 3b). The divergent exercise prescriptions, and their associated effects on the metabolic response to exercise, can be observed by the larger increase in blood lactate concentration following SIT (13-fold; 1.4 ± 0.3 to 18.6 ± 3.5 $mmol \cdot L^{-1}$; $P < 0.001$) when compared to MICT (1.6-fold; 1.38 ± 0.43 to 2.18 ± 0.38 $mmol \cdot L^{-1}$; $P = 0.001$) (Figure 3b; Table S3-Tab 1). Similarly, blood pH levels were only decreased following SIT (from 7.35 ± 0.03 to 7.02 ± 0.09; $P < 0.001$) and not MICT (from 7.35 ± 0.02 to 7.37 ± 0.02; $P > 0.05$) (reflected by fold differences in $[H^+]$ in Figure 3b). These results agree with the well-described effect of exercise intensity on increasing glycolytic flux through anaerobic pathways and the associated increase in lactate and decrease in pH [3, 48]. Immunohistochemical analysis of muscle sections confirmed a greater depletion of muscle glycogen in type I than type II fibres following the first MICT session, and greater muscle glycogen depletion

in the type II fibres following SIT versus MICT (Figure 3c). This is consistent with previous research [49, 50] and demonstrates that the two types of training employed were associated with very different skeletal muscle fibre recruitment patterns (i.e., MICT recruited predominantly type I fibres while SIT recruited both type I & type II fibres; see the schematic in Figure 3d).

We did not detect any significant changes in protein abundance in either fibre type following either training type (Fig 4b; Table S4). While this contrasts with the results of the only published single-fibre proteomic study utilising exercise [30], this discrepancy may be explained by methodological differences between the two studies (e.g., differences in familiarisation, training, and protein quantification methods). The main difference is that we determined statistical significance via an empirical Bayes method (*limma*), while the previous study utilised a posteriori information fusion scheme that combines fold change and statistical significance (unadjusted P value from thousands of individual paired t-tests) [51]. There is good evidence that empirical Bayes methods better control for false positives when analysing large data sets [52]. Indeed, when we reanalysed the data of Deshmukh et al [30], with the same imputation and empirical Bayes methods as our study, we observed no significant changes in protein abundance in either fibre type following their training program (Fig 4c; Table S4). The second notable difference is that the fold changes reported by Deshmukh et al [30] (-4.5 to 3.6 Log_2FC; Fig 4d) were much larger than those observed in our study (-1.5 to 1.7 Log_2FC; Table S4). These larger fold changes may partially be due to differences in quantification methods between our two studies, but would have contributed to the greater number of differences identified via the posteriori information fusion scheme. Thus, our results raise important questions about the ability of human studies with small to moderate sample sizes to confidently detect training-induced changes of individual proteins in single-fibre pools - especially given the inherent inter-individual and inter-fibre variability of human muscle biopsy samples.

Another interesting observation was that there were fewer differentially expressed proteins between type I and type II fibres post-training compared to pre-training (compare Figures 5a & b, Tables S5-Tabs 1 & 2, with Figure 1f). More than 50% of the proteins identified as differentially expressed between type I and type II fibres pre-training were not significantly different post-training (Figure 5d; Table S5-Tab 4). This is consistent with previous reports that type II fibres become more like type I fibres with endurance training [53, 54, 55]. We add that this reduced difference between type I and type II fibres post-training was more pronounced for SIT (greater recruitment of both type I and II fibres; see Figs 3c & d) than MICT. There were, however, an additional 23 differentially expressed proteins between the two fibre types post-MICT that were not differentially expressed between the

two fibre types pre-training (Figure 5d; Table S5-Tab 4). This included Cytochrome b5 reductase (CYB5R3), which was higher in type I fibres following MICT and has recently been linked to the regulation of lipid metabolism and modest lifespan extension in mice [56].

Given the challenges in confidently detecting training-induced changes of individual proteins in human single-fibre pools, we turned our attention to protein groups within different pathways; this allowed for an overview of protein changes within pathways. Network analysis conducted on differentially expressed proteins in the two fibre types after both training interventions (i.e., MICT and SIT) demonstrates that differences were more common between the same fibre type than the same exercise training type (Figure 5f; Table S5-Tab 5 & 6). For example, for both types of training striated muscle contraction proteins associated with slow-twitch skeletal muscle isoforms were predominately higher post-training in type I fibres (TNNT1, TNNI1, TNNC1, TPM3, MYL2 and MYL3), while proteins associated with fast-twitch skeletal muscle isoforms were predominately more abundant post-training in type II fibres (TNNC2, MYH6, TNNT3, MYBPC2, TPM1, TNNI2, MYL1 and MYL4). The network analysis also indicated that proteins associated with glycolysis were mostly differentially expressed only in type II fibres after both types of training; proteins belonging to the glycogen synthesis pathway were only observed to be greater in type II fibres post-MICT and not post-SIT. Finally, although fatty acid oxidation pathway proteins were predominately differentially expressed in type I fibres following training, these differences were all present in the PRE samples.

Fibre-type-specific effects of different types of exercise training on mitochondrial proteins

Mitochondrial content is greater in type I compared with type II fibres [57, 58] (see also Fig 2d). However, while research has reported that markers of mitochondrial content increase with exercise training [6, 59, 60, 61, 62], little is known about the fibre-specific effects of different types of exercise training. Consistent with our morphological (mitochondrial volume density obtained from TEM; Figures 6a & b) and biochemical (citrate synthase [CS] activity; Figure 6c) markers of mitochondrial content (Table S6-Tab 1), we observed a significant increase in the mean abundance of known mitochondrial proteins only following MICT and not SIT (Figure 6d) (Table S6-Tab 2). This can likely be attributed to the five-fold greater volume of training completed by the MICT group [6, 63], although a consensus has yet to be reached on the relative importance of exercise intensity versus volume on training-induced changes in markers of mitochondrial content [61, 64]. Changes in the mean abundance of known mitochondrial proteins following MICT occurred predominantly in the type I

fibres, although there was also a significant but smaller increase in the type II fibres (Figure 6d); this suggests that there is recruitment of type II fibres during long-duration, moderate-intensity exercise. There were no significant increases in known mitochondrial protein abundance in either fibre type following SIT (Figure 6d), although a small decrease was observed in type I fibres.

Given the training-specific changes in the mean abundance of known mitochondrial proteins, we next investigated training-induced changes in the total abundance of proteins in different mitochondrial functional groups in both fibre types. We observed fibre-type-specific adaptations of mitochondrial proteins to training (Figure S1a, Table S8 – Tab 1), consistent with the only other proteomic study investigating the effects of exercise training in pools of single fibres [30]. Our results suggest that the overall mean abundance of many mitochondrial functional groups is enhanced by high-volume, moderate-intensity endurance training. Interestingly, the total abundance of TCA cycle, beta-oxidation, and mitochondrial ribosome proteins increased in both fibre types from PRE to POST MICT (Figures S1b and c, Table S8-Tab 2). This latter result is similar to those of another proteomic study, which revealed changes in mitochondrial ribosomal proteins in whole-muscle samples following interval training [65]. These authors hypothesised that translational level regulation is a predominant factor controlling mitochondrial biogenesis in humans in response to exercise training. No changes in mitochondrial ribosome proteins were observed in either fibre type for SIT. This suggests the volume of MICT was sufficient to induce significant mitochondrial protein synthesis in both fibre types, whereas SIT may not provide a sufficient stimulus to significantly alter mitochondrial protein synthesis [66], and is consistent with our TEM findings (Figure 6b).

Fibre-type-specific expression profiles for mitochondrial proteins independent of training-induced changes in mitochondrial content.

Given the greater changes in mitochondrial content that occur following MICT compared with SIT [60, 67, 68, 69]; see also Figure 6d), we turned our attention to investigating if fibre-type-specific changes in different mitochondrial functional groups with training were independent of changes in total mitochondrial content (MPE). Once again, we employed our normalisation strategy [8] to remove the bias introduced by the changes in mitochondrial content in each fibre type following both types of training (Figure 7a). This enabled us to investigate differences in mitochondrial protein abundances between the two fibre types without the bias introduced by training-induced changes in total mitochondrial content (Table S7 – Tabs 1 & 2). Post normalisation, very few training-induced changes in mitochondrial protein abundances remained in either fibre type, following either training

intervention. One exception was the relative decrease in the abundance of complex IV subunits in both type I and II fibres following SIT (Figure 7b & c). Thus, when changes in mitochondrial content are controlled for, very high-intensity SIT appears to deprioritise the biogenesis of OXPHOS components involved in the final step of the mitochondrial electron transport chain (i.e., complex IV). The other exception was the increase of proteins associated with fatty acid oxidation in type I fibres following MICT, which our results suggest was greater than, and not stoichiometrically linked to, the overall training-induced increase in mitochondrial content (Figure 7d). This adds to the evidence that MICT provides a powerful stimulus to increase fatty acid oxidation [70, 71]; we add that this adaptation occurs predominantly in type I skeletal muscle fibres (with the exercise stimulus employed in our study).

Differences in mitochondrial protein abundance between fibre types is likely due to differences in total mitochondrial content

Proteomics applied to human skeletal muscle remains in its infancy, but has introduced new opportunities to explore the complexity of the biological networks underlying fibre-specific differences and responses to exercise training. In the present study, we developed a sensitive mass spectrometry-based proteomics workflow that allowed for the pooling of single muscle fibres, and the utilisation of tandem mass tag (TMT) labelling, to accommodate our complex experimental design and increase the quantitative accuracy of our results. In addition, we incorporated a larger sample size than previous studies to better account for the individual variability in human skeletal muscle and to increase the robustness of our findings. Consistent with previous research [30], we identified more than 200 differentially expressed proteins between type I and type II fibres at baseline (Figure 1f). However, further analysis of these results allowed us to make two new and important observations. The first is that less than half of mitochondrial proteins (25 of 56) with fibre-type-specific expression profiles remained significantly different when we used our published normalisation strategy to account for the overall greater content of mitochondria in type I versus type II fibres (Figure 2c – bottom panel). Thus, many of the differences in mitochondrial protein abundances between fibre types reported by us (Figure 2c – top panel), and others [29, 30], are likely due to differences in total mitochondrial content rather than representing a fibre-type-specific mitochondrial proteome. A further finding is that more than 50% of the proteins identified as differentially expressed between type I and type II fibres pre-training were not significant post-training (Figure 5d; Table S5-Tab 4). This highlights the challenge of distinguishing between protein

expression profiles intrinsic to different fibre types and those that are a consequence of adaptations to habitual physical activity (or inactivity).

Repeated muscle contractions, via habitual physical activity or exercise training, provide a potent stimulus to alter the expression of proteins and confer many health benefits [4]. The development of mass-spectrometry-based proteomics has advanced our understanding of training-induced changes in protein abundance in mixed-fibre samples [8, 72, 73, 74]. However, while it is well known that adaptations to training depend on the characteristics of the exercise stimulus [10], no proteomic study has investigated the effects of different exercise stimuli on fibre-type-specific adaptations. Therefore, an important feature of our study design was to investigate fibre-type-specific adaptations in response to two types of training that were very different in volume, intensity, metabolic stress, and fibre recruitment patterns (Figure 3). Although our study design was motivated by the many changes reported as significant in the only published single-fibre proteomic study [30], we did not detect any significant changes in the abundance of individual proteins in either fibre type following either training type. Subsequent re-analysis of the previously published data highlighted two potential contributing factors – the greater fold differences reported in the previous study (which may be related to differences in protein quantification method, and/or the choice of imputation method [75]) and the determination of statistical significance via a posteriori information fusion scheme that combines fold change and statistical significance (Figure 4; Table S4). These results collectively highlight some of the methodological challenges that need to be overcome to confidently detect training-induced changes of individual proteins in single-fibre pools - especially given the inherent inter-individual and inter-fibre variability of human muscle biopsy samples.

Given the well-known effects of different types of training on mitochondrial content [68] (see also Figure 6), a further important feature of our study was to investigate whether the fibre-type-specific changes observed by us for the total abundance of proteins in different mitochondrial functional groups were independent of training-induced changes in total mitochondrial content. To do this, we used our previously described normalisation strategy to control for the bias introduced by changes in mitochondrial content in each fibre type following both types of training [8]. This analysis revealed that most training-induced changes in mitochondrial protein abundances were stoichiometrically linked to the overall increase in mitochondrial content (compare Figure 7 with Figure S1). However, a surprising observation was the decrease in the abundance of complex IV subunits, relative to the overall increase in mitochondrial protein content, in both type I and II fibres following SIT. This deprioritisation of the OXPHOS components involved in the final step of the mitochondrial electron

transport chain is intriguing given that, when also controlling for changes in mitochondrial content, we have previously reported greater changes in mitochondrial respiration following SIT than MICT [69]. The results of our novel normalisation strategy also revealed a discordant regulation of proteins associated with fatty acid oxidation, with a non-stoichiometric increase of these proteins in type I but not type II fibres following MICT. A previous study has also reported greater increases in perilipin (PLIN) 2 and 5 in type I compared with type II fibres following MICT [76]. These adaptations may facilitate greater intramuscular triglyceride (IMTG) lipolysis and fatty-acid oxidation in type I fibres when metabolic demand increases [77, 78].

In summary, our study incorporated several unique elements (a sensitive MS-based proteomics workflow, the largest sample size to date, two very different types of training stress, and a novel mitochondrial normalisation strategy) to investigate fibre-specific adaptations to different types of training. This provides an important resource to better understand how different fibre types adapt to different training interventions, with potential insights for how best to prescribe exercise to improve both health and human performance. In contrast to the decreased abundance of complex IV subunits in both type I and II fibres following SIT, and the increase in proteins associated with fatty acid oxidation only in type I fibres with MICT, most training-induced changes in mitochondrial protein abundances were stoichiometrically linked to the overall increase in mitochondrial content.

Limitations of the study

This study recruited healthy, young, active men and, therefore, some of the conclusions may not apply equally well to individuals of different sexes, ages (e.g., the elderly), ethnicity, or health status. Another potential limitation is the use of pooled muscle fibre samples; while this assists in reducing biological variability amongst samples, it may not be a true representation of some single-fibre differences both pre and post-training. It was not possible for us to determine if the fibre-specific adaptations to the two different types of exercise training had functional consequences (e.g., differences in fibre-specific mitochondrial respiratory function). Finally, it is important to note that there are several quantitative mass-spectrometry-based methods used to detect changes in the proteome, each with their advantages and disadvantages, and the results are not always directly comparable.

Resource availability

Lead contact

Further information and requests for reagent and resources may be directed to and will be fulfilled by the lead contact, Professor David J Bishop (David.Bishop@vu.edu.au).

Experimental model and subject details

Participants and ethics approval

Twenty-eight healthy men initially volunteered to take part in this study. The data from sixteen participants (27.5 ± 5.2 y; 177 ± 7 cm; 73.8 ± 8.7 kg; 23.6 ± 2.6 BMI; Table S1 – Tab 1) was included in the final analysis; two participants from the MICT group and two from the SIT group withdrew from the study due to time constraints, and the data from one participant was excluded from the final analysis as their muscle samples were of poor quality. Samples were also excluded where fibre typing by dot blotting was inconsistent with the proteomic data (see study recruitment flow chart and final group sizes; Figure S2f). Participants were provided with the information to participants' document, and were informed of the study requirements, benefits, and risks involved before giving their written informed consent. Ethics approval for the study was obtained from the Victoria University Human Research Ethics Committee (HRE17-075) and was registered as a clinical trial under Australian New Zealand Clinical Trials Registry (ANZCTR; ACTRN12617001105336).

Study design and training. During the first two weeks, participants performed two exercise familiarisation sessions and multiple testing familiarisation sessions. Participants were then allocated into one of the two training groups, based on their age, body mass index (BMI), maximum rate of oxygen consumption (VO_{2max}), peak aerobic power output (W_{max}; $W \cdot kg^{-1}$), and 20-km time trial (TT) performance ($W \cdot kg^{-1}$) (all $P > 0.05$), to match the two groups for baseline endurance characteristics. The participants then underwent another week of testing, had a resting biopsy, and then trained 3 to 4 times per week for 8 weeks before the last muscle biopsy sample and final testing was performed (Figure 3a).

Sprint-Interval Training (SIT).

Eight participants were from this group (28.5 ± 5.9 y; 179 ± 8 cm; 74.2 ± 10.0 kg; 23.3 ± 3.3 BMI; Table S1 – Tab 1). The SIT group completed 4 to 8 30-second "all-out" cycling sprints against a resistance set at 0.075 kg/kg body mass (BM), interspersed with a 4-min recovery period between sprints [69, 79]. The training load was increased to 0.080 $kg \cdot kg^{-1}$ BM in week 3, to 0.085 $kg \cdot kg^{-1}$ BM in week 5, and to 0.090 $kg \cdot kg^{-1}$ BM in week 7. During the recovery, participants remained on the bikes and were allowed to either rest or cycle against no resistance. Participants started the training with 4 sprints per session and this increased up to 8 sprints per session in week 7.

511

Moderate-Intensity Continuous Training (MICT).

Eight participants were from this group (26.5 ± 4.5 y; 176 ± 6 cm; 73.5 ± 7.8 kg; 23.8 ± 1.8 BMI; Table S1 – Tab 1). The training intensity for the MICT training group was established as 10% less than the first lactate threshold (~ 90% of the lactate threshold 1, LT1 - defined as the first increase of ≥ 0.3 $mmol \cdot L^{-1}$ of lactate from the previous stage during the submaximal test). The training intensity prescription was reassessed during the first training session of weeks 3, 5, and 7 and adjusted accordingly. At the commencement of training, participants completed 60 min per session and this increased up to 120 min per session in week 7.

Testing procedures. Participants were required to avoid any vigorous exercise for the 48 h preceding each performance test (72 h for the skeletal muscle biopsy), and to avoid caffeine consumption for at least 8 h prior to each test. Tests were performed at a similar time of the day throughout the study to avoid variations caused by changes in circadian rhythm.

GXT. Graded exercise tests (GXTs) were performed on an electronically braked cycle ergometer (Lode Excalibur v2.0, Groningen, The Netherlands) to determine maximal oxygen uptake ($V\square O_{2max}$) and maximal power ($W\square_{max}$). A GXT design of 1-min incremental stages was utilised, aiming to attain a total testing duration of 9 to 11 minutes. Breath-by-breath recordings of Oxygen Consumption ($V\square O_2$), Expired Carbon Dioxide ($V\square CO_2$), and Ventilatory Efficiency ($V\square_E$) were acquired throughout the GXT using a metabolic analyser (Quark Cardiopulmonary Exercise Testing, Cosmed, Italy). The $W\square_{max}$ was determined as the average power of the last minute completed. After completion of the GXT, there was a 5-min recovery followed by a verification bout performed at an intensity equivalent to 90% of $W\square_{max}$ until task failure to confirm the highest measured $V\square O_{2max}$ [80].

Submaximal test. Once the initial GXT was completed, the ventilatory parameters obtained ($V\square O_2$, $V\square CO_2$, $V\square_E$) were used to estimate the first ventilatory threshold (VT1). Once estimated, the submaximal test started at 40 W lower than the estimated VT1 and the intensity was increased 10 W every 3 min (stage length) until the LT1 was surpassed and identified. The test was stopped at a blood lactate of 2 $mmol \cdot L^{-1}$ as the LT1 had been reached in all cases. Antecubital venous blood was taken in the last 15 s of each stage and was instantly analysed in duplicate using a blood lactate analyser (YSI 2300 STAT Plus, YSI, USA).

Physical activity and nutritional controls. Participants were requested to maintain a normal dietary pattern and physical activity throughout the study. To minimise the variability in muscle metabolism,

participants were provided with a standardised dinner (55 kJ/kg of body mass (BM), providing 2.1 g carbohydrate/kg BM, 0.3 fat/kg BM, and 0.6 g protein/kg BM) and breakfast (41 kJ/kg BM, providing 1.8 g carbohydrate/kg BM, 0.2 g fat/kg BM, and 0.3 g protein/kg BM) to be consumed 15 h and 3 h before the biopsies, respectively.

Muscle biopsies and single muscle fibre isolation. A biopsy needle with suction was used to obtain vastus lateralis muscle biopsies under local anaesthesia (1% xylocaine) at pre training and three days post training. After being cleaned of excess blood, connective tissue, and fat, muscle biopsies were then separated on ice into single fibres. Forty fibres from each biopsy were individually isolated into single fibre segments and then placed in a Laemmli solution (a solubilising buffer) [12]. The Laemmli solution was composed of 4% (v/v) sodium dodecyl sulfate (SDS), a thiol agent of 10% (v/v) ß-mercaptoethanol, 20% (v/v) glycerol, 0.125 M tris-hydroxymethyl-aminomethane (tris)-HCl; and 0.015 % (v/v) bromophenol blue, pH 6.8. Each fibre was diluted with 5 µL of 3x the solubilising buffer 2:1 (v/v) with 10 µL of 1x Tris-Cl (pH 6.8) [12, 23]. These fibre segments were then immediately frozen in liquid nitrogen and stored at ¯80 ºC.

Single Muscle Fibre Analysis – Immunoblotting

Muscle Fibre Typing (Dot Blotting)

To assess muscle fibre types, PVDF membranes were activated in 95% ethanol for 15 to 60 s and then equilibrated for 2 min in transfer buffer (25 mM Tris, 192 mM glycine, pH 8.3 and 20% methanol). The wet membrane was then placed on a stack of filter paper (one to two pieces soaked in transfer buffer on top of one dry piece). The single-fibre samples in the Laemmli solution were then thawed and vortexed, but not centrifuged, to avoid pelleting and hence loss of any of the skeletal muscle protein [12]. Samples were spotted to a specific part of the membrane in aliquots equating to ~ 1/8 of a fibre segment (i.e., 1 µL) using a multi-channel pipette. This was repeated twice, once for type I fibre detection and another time for type II fibre detection. After complete absorption of samples, the membrane was placed on top of a dry piece of filter paper to dry for 2 to 5 min before being reactivated in 95% ethanol for 15 to 60 s and equilibrated in transfer buffer for 2 min. After three quick washes in Tris-buffered saline-Tween (TBST), the membrane was blocked in 5% non-fat milk in TBST (blocking buffer) for 5 min at room temperature. Following blocking, the membrane was rinsed with TBST and then incubated in MYH2 (#A4.74, Developmental Studies Hybridoma Bank [DSHB]) or MYH7 (#A4.840, DSHB) antibody overnight at 4 ºC with gentle rocking. On the second day, membranes were washed in TBST and then incubated in secondary antibody IgG

(MYH2, #A32723, ThermoFisher Scientific) or IgM (MYH7, # Cat # A-21042 4, ThermoFisher Scientific) at room temperature for 1 h with rocking. Lastly, membranes were washed in TBST and then exposed to Clarity-enhanced chemiluminescence reagent (BioRad, Hercules, CA, USA), imaged (ChemiDoc MP, BioRad) and analysed for signal density (ImageLab 5.2.1, BioRad) (see example image in Figure S2i. Using images of all the membranes, it was possible to determine the fibre type of each sample (I or IIa) or if no MHC protein was present [81], which would indicate unsuccessful collection of a fibre segment. Samples with signal density in both type I and IIa membranes were discarded (i.e., a I/IIa hybrid, two different fibre types in the same sample).

Fibre-type pooling

Analysis of how the number of detected proteins changed with increasing pooling is shown in (Figure S2h). An increasing number of peptide and protein identifications was observed with a greater number of pooled fibres. However, there was little change in the number of detections from 6 to 9 fibre segments and the number of proteins identified plateaued beyond 6 fibres. A fixed fibre pooling of 6 fibre segments was chosen for this study to allow for sufficient protein coverage and to provide reduced heterogeneity with the same number of pooling across all samples. In addition, this was the maximum number of pooled fibres available for some participants.

Muscle glycogen fibre-type histochemistry analysis

Muscles were embedded in O.C.T. compound (Tissue-Tek), frozen in liquid nitrogen-cooled isopentane, stored at ¯80 °C, and subsequently cut into 10 µm thick cryosections with a cryostat (Leica) maintained at −20 °C.

Fibre type-specific glycogen depletion was imaged under brightfield using periodic acid-Schiff stain (PAS), similar to the methodology described elsewhere [82]. As such, 10 µm thick muscle cryosections were serially sectioned onto cleaned glass slides and subsequently fixed in 3.7% formaldehyde in 90% ethanol for 60 min at 4˚C. After this fixation, sections were then pre-treated for 5 min with 1% periodic acid (Sigma-Aldrich, Australia) in milliQ-water followed by a washing step for 1 min in tap water and a wash dip for 5 s in milliQ-water. The slides were then applied with 15% diluted Schiff's reagent in PBS (Sigma-Aldrich, Australia) and incubated for 15 min at room temperature. The Schiff's reagent was diluted to 15% based on prior optimisation, as when applied without any dilution the dye intensity saturated the signal. After Schiff's reagent, the sections were washed for 5 s in milliQ-water followed by a 10-min rinse with tap water. Thereafter, sections were washed (3 x 5 min) in PBS (137 mmol.L^{-1} sodium chloride, 3 mmol.L^{-1} potassium chloride, 8 mmol.L^{-1} sodium

phosphate dibasic and 3 mmol.L^{-1} potassium phosphate monobasic, pH of 7.4). Slides were then dried before adding ~ 15 µL of PBS per section and mounting with cover slips. The slides were then viewed and imaged in high resolution using an Olympus BX51 fluorescence microscope (Olympus Corporation, Tokyo, Japan) and Cell F software (Olympus). All images were obtained with the x10 objective and captured under bright-field mode.

The second serially sectioned slide underwent immunofluorescence staining for MHC expression and was performed with 1:25 primary antibodies against MHCI (BA-F8) and MHCIIa (BF-35) (Developmental Studies Hybridoma Bank, University of Iowa), whereas secondary antibodies were Alexa fluor 350 IgG_{2b} 1:500 (blue) and Alexa fluor 488 IgG_{2b} 1:500 (green) (Invitrogen). Antibody cocktail configurations and immunofluorescence staining procedures were followed according to Bloemberg et al. [83]. Once completely dry, the sections were incubated (blocked) with 10% goat serum (product no: 50197Z, ThermoFisher Scientific) for one hour. The excess goat serum was then removed, and sections were incubated with primary fibre type antibodies over night at 4 ºC. The following morning, the primary antibodies were washed off in milliQ water (3 x 5 minutes). Once the slides were fully dry, they were incubated with fluoro-conjugated secondary antibodies for 90 minutes. Slides were washed further with milliQ water (3 x 5 minutes) post incubation and dried before adding ~ 15 µL of PBS per section and mounting with cover slips. The slides were then viewed and imaged in high resolution using an Olympus BX51 fluorescence microscope (Olympus Corporation, Tokyo, Japan) and Cell F software (Olympus). All images were obtained with the x10 objective and analysis of images was performed using Image J software (National Institutes of Health, Maryland, USA) (See Figure 3a for example images).

Citrate Synthase (CS) Activity Assay.

Citrate Synthase activity was analysed on a 96-well plate by combining 5 µL of a 2 $\mu g \cdot \mu L^{-1}$ muscle lysate, 40 µL of 3 mM acetyl CoA, and 25 µL of 1 mM DTNB to 165 µL of 100 mM Tris buffer (pH 8.3). Following this, 15 µL of 10 mM oxaloacetic acid was added to the plate mixture, protected from the light, and immediately placed in the spectrophotometer at 30 °C (xMark Microplate Spectrophotometer, Bio-Rad Laboratories Pty Ltd, Gladesville, NSW, AUS). Absorbance was recorded at 412 nm every 15 s for 6 min after 30 s of mixture agitation. CS activity was calculated from the steepest part of the curve and reported as $mol \cdot kg\ protein^{-1} \cdot h^{-1}$.

Blood Lactate and pH measurements

Antecubital venous blood samples (~ 1 mL) were collected pre and post the first exercise training session from a cannula inserted in the antecubital vein for the determination of venous blood [H^+] and lactate concentrations using a blood-gas analyser (ABL 800 FLEX, Radiometer Copenhagen).

Transmission Electron Microscopy.

Skeletal muscle samples were fixed overnight at 4 °C with 0.2 M sodium cacodylate– buffered, 2.5% glutaraldehyde, and 2% paraformaldehyde. Fixed samples were rinsed with 0.1 M sodium cacodylate, and postfixed with ferricyanide-reduced osmium tetroxide (1% OsO4, 1.5% K3 [Fe(CN)6], and 0.065 M cacodylate buffer) for 2 h at 4°C. The postfixed samples, were processed by the Monash Ramaciotti Centre for Cryo-Electron Microscopy, were rinsed with distilled water and then stored overnight in 70% ethanol. Dehydration was performed by graduated ethanol series (80%, 90%, 95%, 100%, and 100%; 10 min each) and propylene oxide (100% and 100%; 5 min each). Samples were infiltrated with Araldite 502/Embed 812 by graduated concentration series in propylene oxide (25% for 1 h, 33% for 1 h, 50% overnight; 66% for 4 h, 75% for 4 h, 100% overnight; and 100% for 5 h) and then polymerised at 60 °C for 48 h. Embedded samples were sectioned using an Ultracut UCT ultramicrotome (Leica Biosystems) equipped with a 45° diamond knife (Diatome) to cut 75-nm ultrathin sections. The grids were stained at room temperature using 2% aqueous uranyl acetate (5 min) and Reynolds lead citrate (3 min) before routine imaging. All TEM imaging was performed at 80 kV on a Jeol JEM-1400Plus and recorded with a Matataki flash camera and DigitalMicrograph (Version 1.71.38) acquisition software.

Proteome Sample preparation

Fibres were placed into 5 µL of 2x SDS solubilising buffer (0.125 M Tris·Cl, pH 6.8, 4% SDS, 10% glycerol, 4 M urea, 5% mercaptoethanol, 0.001% bromophenol blue) diluted 2 times (vol/vol) with 1 x Tris·Cl, pH 6.8. Fibres were pooled according to fibre type and further lysed with heating at 95 °C for 10 min. The pooled fibres were then sonicated for 20 min (Bioruptor, Diagenode, 20 cycles of 30 s). Reduction and alkylation of disulfides was performed by adding chloroacetamide (40 mM, CAA, Sigma) and further incubated for 30 min at 50 °C. The SDS lysate was acidified with 12% aqueous phosphoric acid at 1:10 for a final concentration of ~ 1.2% phosphoric acid and mixed. This step was essential as the proteins are filtered at this pH. The high percentage of methanol can then precipitate the protein out, which will be retained on top of the S-Trap™ (ProtiFi). Following this, 350 µL of S-Trap™ buffer (90% Methanol (MeOH) and 100 mM triethylammounium bicarbonate (TEAB),

$C_7H_{17}NO_3$) was added to the acidified lysis buffer (final pH 7.1). A colloidal protein particulate was instantly formed in this step. With the S-Trap™ micro column in a 1.7 mL tube for flow through, the acidified SDS lysate/MeOH S-Trap™ buffer mixture was added into the micro column. The micro column was then centrifuged at 6500 rpm for 30 s until all SDS lysate/ S-Trap™ buffer had passed through the S-Trap™ column. Protein was then trapped within the protein-trapping matrix of the spin column. The captured protein was then washed with 350 µL S-Trap™ buffer with centrifugation and washing repeated three times. The spin column was then transferred to a fresh 1.7 mL tube (this aided in preventing contamination of the digestion). For best results, the S-Trap™ micro column was rotated 180 degrees between the centrifugation washes. The S-Trap™ micro column was then moved to a clean 1.7 mL sample tube for the digestion with the protease (trypsin and LysC added at a concentration of 1:50 in 125 µL of 50 mM digestion buffer) into the top of the micro column. The sample was then centrifuged at a low speed of 1000 rpm for 30 s and any solution that passes through is returned to the top of the column (the protein-trapping matrix is highly hydrophilic and will absorb the solution; however, it was important to ensure there was no bubble at the top of the protein trap). The column was then transferred to another fresh tube and incubated at 37 °C overnight (~ 16 hours). For 96-well plates, the protease combination was added at a concentration of 1:25 in 125 µL of 50 mM digestion buffer and incubated for 1 hour at 47 °C.

Peptides were eluted with 80 µL each of digestion buffer (50 mM TEAB) and then 0.2% aqueous formic acid was added to the S-Trap™ protein trapping matrix centrifuged at 3600 rpm for 60 s for each elution. Hydrophobic peptides were recovered with an elution of 80 µL 60% (v/v) acetonitrile containing 0.2% formic acid and then centrifuged at 6500 rpm for 60 s. Elutions were pooled.

Further peptide purification was performed as required with 2x SDB-RPS disc stage tips that were prepared and had sample loaded onto the stage-tip. Peptides were then centrifuged through the column at 1500 g for 3 min. Stage tips were washed with 100 uL of 90% isopropanol (C_3H_8O) containing 1% TFA and then washed again with 0.2% TFA in 5% acetonitrile and centrifuged for 4 min following each wash. Peptides were then eluted by adding 100 uL of 60% acetonitrile containing 5% ammonium hydroxide and centrifuged for 4 min. Samples were lyophilised down to dryness with the SpeedVac (CentriVap Benchtop Centrifugal Vacuum Concentrator, # 7810038, VWR) and reconstituted for labelling and subsequent MS analysis.

TMTpro Labelling

TMTpro Label Reagents (ThermoFisher) were equilibrated to room temperature and 20 µL of anhydrous acetonitrile was added to each tube. Dried samples were reconstituted in 0.5 M HEPES buffer, pH 8.5. The desired amount of TMTpro label was added and incubated at 20 °C for 1 h with shaking (1000 rpm). The reaction was then quenched by adding a final concentration of 0.25% of hydroxylamine to the peptide and TMT mixture, and further incubated at 20 °C for 30 min. Samples were lyophilised down to dryness with the SpeedVac and reconstituted in loading buffer. Each sample was fractionated into 16 fractions using basic pH reverse phase C18 liquid chromatography. Peptides were subjected to basic-pH reverse-phase high pressure liquid chromatography (HPLC) fractionation. Labelled peptides were solubilised in buffer A (10 mM ammonium hydroxide) and separated on an Agilent HpH Poroshell120 C18 column (2.7 µm particles, 2.1 mm i.d., and 5 cm in length).

TMT Labelling Strategy

Multiplexing techniques have recently extended from 11 to 16 plex, which not only increases sample throughput but accommodates complex experimental designs such as this training study. This provided the ability to label 16 samples in one run and then merge as one sample through the LC-MS. A 16-plex also allows for an expanded number of treatments, such as replicates, and dose-response or time-course measurements can be analysed in the same experiment with basically no missing values across all samples and extending the statistical power across the entire system [84]. The main study used TMTpro 16-plex version with a different reporter and mass normaliser than earlier TMT versions (i.e., TMT-6 plex). A limitation of tag-based proteomic strategies is ion interference-related ratio distortion resulting from fragmentation and analysis of background ions co-isolated with those of interest. Each sample is differentially labelled, such that when pooled the signal-to-noise values of sample-specific reporter ions represent the relative abundance of each protein. As such, the degree of ion interference by the level of TMT signal detected in channels where a specific protein should be absent can be assessed [85]. Our sampling strategy was adopted to best accommodate for possible reporter ion interferences. Reporter ion interference (RII) targets were classified according to a typical product data sheet for 16-plex TMTpro Label Reagents from ThermoFisher Scientific.

Liquid Chromatography-MS/MS Acquisition

Peptides were loaded onto a 2-cm PepMap trap column (ThermoFisher) and separated using a PepMap 75 µm × 50 cm column (ThermoFisher) with a gradient of 2–30% MeCN containing 0.1% FA over 120 min at 250 nL/min and at 40 °C. The Orbitrap Fusion mass spectrometer was operated

with the following parameters: an MS1 scan was acquired from 375–1575 m/z (120,000 resolution, 2e5 AGC, 50 ms injection time) followed by MS2 data-dependent acquisition with collision-induced dissociation (CID) and detection in the ion trap (4e3 AGC, 150 ms injection time, 30 NCE, 1.6 m/z quadrupole isolation width, 0.25 activation Q). To quantify TMTpro reporter ions, a synchronous precursor selection MS3 scan was performed with higher-energy collisional dissociation (HCD) and detection in the orbitrap (120 to 750 m/z, 1e5 AGC, 250 ms injection time, 60 NCE, 2.5 m/z isolation width). The total cycle time was set to 2.5 s. The acquired raw data was analysed with Proteome Discoverer 2.4 (ThermoFisher) and the non-normalised protein reporter intensity was exported to Excel and further analysed in R.

Bioinformatic analysis of proteomics data.

Clean up and normalisation

Only proteins that had a high FDR confidence, were not deemed a contaminant, and had greater than one unique peptide, were used for analysis. Proteins having < 70% valid values were removed and the remaining missing data was imputed using k nearest neighbour (knn) method from the *impute* package in R. Normalisation was performed using a combination of trimmed mean of M values (TMM), sample loading (SL), and ComBat (v0.0.4) methods [86, 87, 88, 89]. Sample loading adjusts each TMT experiment to an equal signal per channel and TMM uses the average or median signal that is typically applied to use a single multiplicative factor to further adjust the samples to each other. Further to this, ComBat allows users to adjust for batch effects in datasets where the batch covariate is known, using previously described methodology [87].

Differential expression analysis

Differential expression analysis was performed using the R package *limma* (v3.48.3) [90] on the relative protein abundances after first performing the normalisation technique described above. Differential expression values were determined by comparing relative protein abundances. To focus on proteins specifically associated with fibre type, the differential expression comparisons were first filtered to include proteins differentially expressed between type I and type II fibres before exercise (adjusted P value < 0.05). This established the baseline of the proteins that were significantly different between the two fibre types prior to exercise and allowed for comparisons between our data and the data of Murgia et. al. (2017) and Deshmukh et. al. (2020) (Figures 1 and 2). Following this, comparisons were made to identify any significant effects (Fusion Factor P value < 0.05) exercise produced on each of the fibre types for each type of exercise (MICT type I Pre vs Post, MICT type II

Pre vs Post, SIT type I Pre vs Post, SIT type II Pre vs Post; Figure 4). Finally, comparisons were completed between fibre types on samples post exercise (MICT Post type I vs type II and SIT Post type I vs type II, Figure 4), to distinguish and compare significant (adjusted P value < 0.05) differences between the fibre types after exercise. Mitochondrial proteins were identified by annotation using both the Integrated Mitochondrial Protein Index (IMPI) and the Mitocarta 3.0 database [91].

The heatmap presented in Figure 1g was completed using the *ComplexHeatmap* package (v.2.8.0), with hierarchical clustering using the "average" method. The heatmap presented in Figure 7c was created using the native R heatmap function and clustered according to the OXPHOS complex subunits as identified in MitoCarta 3.0. For visualisations of differential expression comparisons, volcano plots were presented in Figure 1f, 2e & f, 5a & b and used the resulting adjusted P values from the *limma* analysis, which can be found in Table S1, S2, S3 and S4. Volcanos from Figure 4 b and c used the P values from the Fusion Factor calculation found in Table S4. Profile Plots presented in Figures 6d, 7a,b,d and S1b,c, were created by calculating a mean of the group in question (complex or functional group as identified by MitoCarta 3.0) with all proteins identified in that group coloured and a background displayed of all mitochondrial proteins (with an exception for Figure 7a, which used all proteins identified). Statistical significance between Pre and Post training values within the profile plots was completed using a paired t-test and the default adjustment for multiple hypothesis testing. Venn diagrams featured in Figure 1c, 2a were created using the *VennDiagram* (v1.7.1) package.

To better characterise the proteomic changes, gene ontology and enrichment analysis were performed by investigating non-random associations between proteins and over-represented Gene Ontology (GO). For Figure 1b, we calculated the average number of proteins in each pooled sample, the proteins identified within the entire dataset of high confidence proteins and compared them to the entire human genome to determine how many were identified in specific GO CC terms compared to the human genome. Figure 1d and 2b compared the 844 and 314 proteins that were common between the three datasets investigated and the top five GO CC terms for the 844 proteins were visualised, with the top five GO BP terms used for the 314. These analyses were conducted using Database for Annotation, Visualization and Integrated Discovery (DAVID) [92]. Network plots and WikiPathways are presented in Figure 5e and 5f respectively. The network plot (Figure 5f) was completed using only statistically significant (adjusted P value < 0.05) results for the comparisons of type I vs II

values post both MICT and SIT, whereas the Wikipathways BubblePlot uses all results for the same comparisons. These analyses were completed using the R package *ClusterProfiler* (v4.0.5).

Mitochondrial Normalisation

As the mitochondrial protein expression identified a difference in the mitochondrial content between the two fibre types before exercise, we employed a previously reported normalisation strategy [8]. This normalisation strategy removes bias introduced by the differences in mitochondrial content and allows the investigation of these adaptations when this bias was removed. Mitochondrial proteins identified through IMPI and MitoCarta 3.0 were subset from the rest of the data, and the same normalisation protocol as reported above was applied.

Data availability and code availability

- Source data to interpret, verify, and extend this research is provided with this paper. The mass spectrometry proteomics data has been deposited in the ProteomeXchange Consortium via the PRIDE partner repository under accession code PXD036010.

- The R scripts used for all omics analyses described above are deposited on GitHub and available through https://doi.org/10.5281/zenodo.7227800. There are no restrictions placed on accessibility of this code.

Author Contributions Statement

D.J.B., J.B, E.R., and C.G. conceptualised and designed the study. J.B. carried out the training study and sample collection. E.R., J.B., and C.H. performed the experiments. E.R and S.C. performed muscle glycogen fibre-type histochemistry analysis. V.O and G.R. performed the electron microscopy experiments. N. J. C. performed the statistical and bioinformatic analysis. D.J.B., E.R., and N.J.C. wrote the manuscript. E.R., J.B., C.H, R.B.S. D.A.S, C.G., N.J.C and D.J.B. edited and revised the manuscript. All persons designated as authors qualify for authorship, and all those qualifying for authorship are listed. All authors have read and approved the final manuscript.

Acknowledgments

We thank Iresha Hanchapola from Monash Proteomics & Metabolomics Facility for proteomic supplies and instrument support and acknowledge Associate Professor Javier Diaz Lara from the University de Navarra for support with dot blotting.

Funding

This study was supported by grants from the Australian Research Council (Discovery Projects DP140104165 and DP200103542 to D.J.B), the Australian Physiological Society (Ph.D. grant to J.B), and the Australian National Health and Medical Research Council (NHMRC Fellowship GNT2009732 to D.A.S.). J.B. was supported by a Victoria University International Postgraduate Research Scholarship.

Competing Interests Statement

The authors declare no conflict of interest.

References

1. Egan B, Zierath JR. Exercise metabolism and the molecular regulation of skeletal muscle adaptation. *Cell Metab* **17**, 162-184 (2013).

2. Hawley JA, Hargreaves M, Joyner MJ, Zierath JR. Integrative biology of exercise. *Cell* **159**, 738-749 (2014).

3. Hargreaves M, Spriet LL. Skeletal muscle energy metabolism during exercise. *Nature Metabolism* **2**, 817-828 (2020).

4. Neufer PD, *et al.* Understanding the Cellular and Molecular Mechanisms of Physical Activity-Induced Health Benefits. *Cell Metabolism* **22**, 4-11 (2015).

5. Miller BF, Hamilton KL. A perspective on the determination of mitochondrial biogenesis. *American journal of physiology Endocrinology and metabolism* **302**, E496-E499 (2012).

6. Bishop DJ, *et al.* High-Intensity Exercise and Mitochondrial Biogenesis: Current Controversies and Future Research Directions. *Physiology* **34**, 56-70 (2018).

7. Saner NJ, *et al.* Exercise mitigates sleep-loss-induced changes in glucose tolerance, mitochondrial function, sarcoplasmic protein synthesis, and diurnal rhythms. *Molecular Metabolism* **43**, 101110 (2021).

8. Granata C, *et al.* High-intensity training induces non-stoichiometric changes in the mitochondrial proteome of human skeletal muscle without reorganisation of respiratory chain content. *Nature Communications* **12**, 7056 (2021).

9. Holloszy JO, Coyle EF. Adaptations of skeletal muscle to endurance exercise and their metabolic consequences. *Journal of applied physiology: respiratory, environmental and exercise physiology* **56**, 831-838 (1984).

10. Jamnick NA, Pettitt RW, Granata C, Pyne DB, Bishop DJ. An Examination and Critique of Current Methods to Determine Exercise Intensity. *Sports Medicine,* (2020).

11. MacInnis MJ, Gibala MJ. Physiological adaptations to interval training and the role of exercise intensity. *J Physiol* **595**, 2915-2930 (2017).

12. Murphy RM. Enhanced technique to measure proteins in single segments of human skeletal muscle fibers: fiber-type dependence of AMPK-alpha1 and -beta1. *Journal of applied physiology (Bethesda, Md : 1985)* **110**, 820-825 (2011).

13. Howald H, Hoppeler H, Claassen H, Mathieu O, Straub R. Influences of endurance training on the ultrastructural composition of the different muscle fiber types in humans. *Pflugers Archiv : European journal of physiology* **403**, 369-376 (1985).

14. Ingjer F. Effects of endurance training on muscle fibre ATP-ase activity, capillary supply and mitochondrial content in man. *The Journal of Physiology* **294**, 419-432 (1979).

15. Kiessling KH, Pilström L, Bylund AC, Saltin B, Piehl K. Enzyme Activities and Morphometry in Skeletal Muscle of Middle-Aged Men after Training. *Scandinavian journal of clinical and laboratory investigation* **33**, 63-69 (1974).

16. Jackman MR, Willis WT. Characteristics of mitochondria isolated from type I and type IIb skeletal muscle. *American Journal of Physiology-Cell Physiology* **270**, C673-C678 (1996).

17. Henneman E, Olson CB. Relations Between Structure and Function in the Design of Skeletal Muscle. *Journal of Neurophysiology* **28**, 581-598 (1965).

18. Vollestad NK, Blom PC. Effect of varying exercise intensity on glycogen depletion in human muscle fibres. *Acta Physiol Scand* **125**, 395-405 (1985).

19. Sale DG. Influence of exercise and training on motor unit activation. *Exercise and sport sciences reviews* **15**, 95-151 (1987).

20. Henneman E. Relation between Size of Neurons and Their Susceptibility to Discharge. *Science (New York, NY)* **126**, 1345 (1957).

21. Mendell LM. The size principle: a rule describing the recruitment of motoneurons. *Journal of Neurophysiology* **93**, 3024-3026 (2005).

22. Dudley GA, Abraham WM, Terjung RL. Influence of exercise intensity and duration on biochemical adaptations in skeletal muscle. *Journal of applied physiology: respiratory, environmental and exercise physiology* **53**, 844-850 (1982).

23. Wyckelsma VL, *et al.* Single-fiber expression and fiber-specific adaptability to short-term intense exercise training of Na+-K+-ATPase α- and β-isoforms in human skeletal muscle. *Journal of Applied Physiology* **118**, 699-706 (2015).

24. MacInnis MJ, *et al.* Superior mitochondrial adaptations in human skeletal muscle after interval compared to continuous single-leg cycling matched for total work. *The Journal of Physiology* **595**, 2955-2968 (2017).

25. Tan R, *et al.* Skeletal muscle fiber-type-specific changes in markers of capillary and mitochondrial content after low-volume interval training in overweight women. *Physiological reports* **6**, (2018).

26. Skelly LE, *et al.* Human skeletal muscle fiber type-specific responses to sprint interval and moderate-intensity continuous exercise: acute and training-induced changes. *Journal of applied physiology (Bethesda, Md : 1985)* **130**, 1001-1014 (2021).

27. Kristensen DE, Albers PH, Prats C, Baba O, Birk JB, Wojtaszewski JF. Human muscle fibre type-specific regulation of AMPK and downstream targets by exercise. *J Physiol* **593**, 2053-2069 (2015).

28. Murgia M, ,, *et al.* Single muscle fiber proteomics reveals unexpected mitochondrial specialization. *EMBO Reports* **16**, 387-395. (2015).

29. Murgia M, *et al.* Single Muscle Fiber Proteomics Reveals Fiber-Type- Specific Features of Human Muscle Aging *Cell Reports* **19**, 2396–2409 (2017).

30. Deshmukh AS, *et al.* Deep muscle-proteomic analysis of freeze-dried human muscle biopsies reveals fiber type-specific adaptations to exercise training. *Nature Communications* **12**, 304 (2021).

31. Suriano R, Edge J, Bishop D. Effects of cycle strategy and fibre composition on muscle glycogen depletion pattern and subsequent running economy. *Br J Sports Med* **44**, 443-448 (2010).

32. Ohlendieck K. Proteomics of skeletal muscle differentiation, neuromuscular disorders and fiber aging. *Expert review of proteomics* **7**, 283-296 (2010).

33. Ohlendieck K. Proteomics of exercise-induced skeletal muscle adaptations. *OA Sports Medicine* **1**, 1-12 (2013).

34. Deshmukh AS, Murgia M, Nagaraj N, Treebak JT, Cox J, Mann M. Deep Proteomics of Mouse Skeletal Muscle Enables Quantitation of Protein Isoforms, Metabolic Pathways, and Transcription Factors *Molecular and Cell Proteomics* **14**, 841-853 (2015).

35. Galpin AJ, *et al.* Human skeletal muscle fiber type specific protein content. *Analytical biochemistry* **425**, 175-182 (2012).

36. Ohlendieck K. Skeletal muscle proteomics: current approaches, technical challenges and emerging techniques. *Skeletal Muscle* **1**, 1-15 (2011).

37. Pappireddi N, Martin L, Wühr M. A Review on Quantitative Multiplexed Proteomics. *Chembiochem* **20**, 1210-1224 (2019).

38. O'Connell JD, Paulo JA, O'Brien JJ, Gygi SP. Proteome-Wide Evaluation of Two Common Protein Quantification Methods. *Journal of proteome research* **17**, 1934-1942 (2018).

39. Schiaffino S, Rossi AC, Smerdu V, Leinwand LA, Reggiani C. Developmental myosins: expression patterns and functional significance. *Skeletal Muscle* **5**, 22 (2015).

40. Morissette MP, *et al.* Differential regulation of the fiber type-specific gene expression of the sarcoplasmic reticulum calcium-ATPase isoforms induced by exercise training. *Journal of applied physiology (Bethesda, Md : 1985)* **117**, 544-555 (2014).

41. Lamboley CR, Wyckelsma VL, Dutka TL, McKenna MJ, Murphy RM, Lamb GD. Contractile properties and sarcoplasmic reticulum calcium content in type I and type II skeletal muscle fibres in active aged humans. *J Physiol* **593**, 2499-2514 (2015).

42. Schiaffino SaR, C. Fiber Types in Mammalian Skeletal Muscles. *Physiol Rev* **91**, 1447–1531 (2011).

43. Sahlin K, Mogensen M, Bagger M, Fernström M, Pedersen PK. The potential for mitochondrial fat oxidation in human skeletal muscle influences whole body fat oxidation during low-intensity exercise. *Am J Physiol Endocrinol Metab* **292**, E223-230 (2007).

44. Ørtenblad N, Nielsen J, Boushel R, Söderlund K, Saltin B, Holmberg H-C. The Muscle Fiber Profiles, Mitochondrial Content, and Enzyme Activities of the Exceptionally Well-Trained Arm and Leg Muscles of Elite Cross-Country Skiers. *Frontiers in physiology* **9**, 1031-1031 (2018).

45. Kiessling KH, Piehl K, Lundquist CG. Effect of Physical Training on Ultrastructural Features in Human Skeletal Muscle. In: *Muscle Metabolism During Exercise: Proceedings of a Karolinska Institutet Symposium held in Stockholm, Sweden, September 6–9, 1970 Honorary guest: E Hohwü Christensen* (eds Pernow B, Saltin B). Springer US (1971).

46. Godin R, Ascah A, Daussin FN. Intensity-dependent activation of intracellular signalling pathways in skeletal muscle: role of fibre type recruitment during exercise. *J Physiol* **588**, 4073-4074 (2010).

47. Greenhaff PL, *et al.* The metabolic responses of human type I and II muscle fibres during maximal treadmill sprinting. *The Journal of Physiology* **478**, 149-155 (1994).

48. van Loon LJ, Greenhaff PL, Constantin-Teodosiu D, Saris WH, Wagenmakers AJ. The effects of increasing exercise intensity on muscle fuel utilisation in humans. *The Journal of physiology* **536**, 295-304 (2001).

49. Scribbans TD, *et al.* Fibre-specific responses to endurance and low volume high intensity interval training: striking similarities in acute and chronic adaptation. *PLoS One* **9**, e98119 (2014).

50. Gollnick PD, Piehl K, Saltin B. Selective glycogen depletion pattern in human muscle fibres after exercise of varying intensity and at varying pedalling rates. *J Physiol* **241**, 45-57 (1974).

51. Xiao Y, *et al.* A novel significance score for gene selection and ranking. *Bioinformatics* **30**, 801-807 (2014).

52. Kelter R. Analysis of type I and II error rates of Bayesian and frequentist parametric and nonparametric two-sample hypothesis tests under preliminary assessment of normality. *Computational Statistics* **36**, 1263-1288 (2021).

53. Wilson JM, Loenneke JP, Jo E, Wilson GJ, Zourdos MC, Kim JS. The effects of endurance, strength, and power training on muscle fiber type shifting. *J Strength Cond Res* **26**, 1724-1729 (2012).

54. Jansson E, Sjodin B, Tesch P. Changes in muscle fibre type distribution in man after physical training. A sign of fibre type transformation? *Acta Physiol Scand* **104**, 235-237 (1978).

55. Bergh U, Thorstensson A, Sjödin B, Hulten B, Piehl K, Karlsson J. Maximal oxygen uptake and muscle fiber types in trained and untrained humans. *Med Sci Sports* **10**, 151-154 (1978).

56. Martin-Montalvo A, *et al.* Cytochrome b5 reductase and the control of lipid metabolism and healthspan. *npj Aging and Mechanisms of Disease* **2**, 16006 (2016).

57. Glancy B, Balaban RS. Protein composition and function of red and white skeletal muscle mitochondria. *American journal of physiology Cell physiology* **300**, C1280-C1290 (2011).

58. Leary SC, Lyons CN, Rosenberger AG, Ballantyne JS, Stillman J, Moyes CD. Fiber-type differences in muscle mitochondrial profiles. *American Journal of Physiology-Regulatory, Integrative and Comparative Physiology* **285**, R817-R826 (2003).

59. Morgan TE, Cobb LA, Short FA, Ross R, Gunn DR. Effects of Long-Term Exercise on Human Muscle Mitochondria. In: *Muscle Metabolism During Exercise: Proceedings of a Karolinska Institutet Symposium held in Stockholm, Sweden, September 6–9, 1970 Honorary guest: E Hohwü Christensen* (eds Pernow B, Saltin B). Springer US (1971).

60. Bishop DJ, Granata C, Eynon N. Can we optimise the exercise training prescription to maximise improvements in mitochondria function and content? . *Biochimica et Biophysica Acta* **1840**, 1266–1275 (2014).

61. Bishop DJ, Botella J, Granata C. CrossTalk opposing view: Exercise training volume is more important than training intensity to promote increases in mitochondrial content. *The Journal of Physiology* **0**, (2019).

62. Larsen S, *et al.* Biomarkers of mitochondrial content in skeletal muscle of healthy young human subjects. *J Physiol* **590**, 3349-3360 (2012).

63. Granata C, Jamnick NA, Bishop DJ. Training-Induced Changes in Mitochondrial Content and Respiratory Function in Human Skeletal Muscle *Sports Medicine* **48**, 1809-1828 (2018).

64. MacInnis MJ, Skelly LE, Gibala MJ. CrossTalk proposal: Exercise training intensity is more important than volume to promote increases in human skeletal muscle mitochondrial content. *J Physiol* **597**, 4111-4113 (2019).

65. Robinson MM, *et al.* Enhanced Protein Translation Underlies Improved Metabolic and Physical Adaptations to Different Exercise Training Modes in Young and Old Humans. *Cell Metab* **25**, 581-592 (2017).

66. Scalzo RL, *et al.* Greater muscle protein synthesis and mitochondrial biogenesis in males compared with females during sprint interval training. *Faseb j* **28**, 2705-2714 (2014).

67. Granata C, Oliveira RSF, Little JP, Renner K, Bishop DJ. Mitochondrial adaptations to high-volume exercise training are rapidly reversed after a reduction in training volume in human skeletal muscle *The Federation of American Societies for Experimental Biology Journal* **30**, 1-11 (2016).

68. Granata C, Jamnick NJ, Bishop DJ. Training-induced mitochondrial adaptations. *Sports Med*, 1-20 (2018).

69. Granata C, Oliveira RS, Little JP, Renner K, Bishop DJ. Training intensity modulates changes in PGC-1α and p53 protein content and mitochondrial respiration, but not markers of mitochondrial content in human skeletal muscle. *Faseb j* **30**, 959-970 (2016).

70. Shaw CS, *et al.* The impact of exercise training status on the fibre type specific abundance of proteins regulating intramuscular lipid metabolism. *Journal of Applied Physiology*, (2020).

71. Martin WH, 3rd, *et al.* Effect of endurance training on plasma free fatty acid turnover and oxidation during exercise. *The American journal of physiology* **265**, E708-714 (1993).

72. Egan B, *et al.* 2-D DIGE analysis of the mitochondrial proteome from human skeletal muscle reveals time coursedependent remodelling in response to 14 consecutive days of endurance exercise training *Proteomics* **11**, 1413–1428 (2011).

73. Holloway KV, *et al.* Proteomic investigation of changes in human vastus lateralis muscle in response to interval-exercise training. *Proteomics* **9**, 5155-5174 (2009).

74. Hostrup M, Onslev J, Jacobson GA, Wilson R, Bangsbo J. Chronic β2-adrenoceptor agonist treatment alters muscle proteome and functional adaptations induced by high intensity training in young men. *The Journal of Physiology* **596**, 231-252 (2018).

75. Lazar C, Gatto L, Ferro M, Bruley C, Burger T. Accounting for the Multiple Natures of Missing Values in Label-Free Quantitative Proteomics Data Sets to Compare Imputation Strategies. *Journal of Proteome Research* **15**, 1116-1125 (2016).

76. Shepherd SO, *et al.* Lipid droplet remodelling and reduced muscle ceramides following sprint interval and moderate-intensity continuous exercise training in obese males. *International Journal of Obesity* **41**, 1745-1754 (2017).

77. Shepherd SO, *et al.* Sprint interval and traditional endurance training increase net intramuscular triglyceride breakdown and expression of perilipin 2 and 5. *J Physiol* **591**, 657-675 (2013).

78. Shepherd SO, *et al.* Preferential utilization of perilipin 2-associated intramuscular triglycerides during 1 h of moderate-intensity endurance-type exercise. *Experimental physiology* **97**, 970-980 (2012).

79. Gillen JB, Martin BJ, MacInnis MJ, Skelly LE, Tarnopolsky MA, Gibala MJ. Twelve Weeks of Sprint Interval Training Improves Indices of Cardiometabolic Health Similar to Traditional Endurance Training despite a Five-Fold Lower Exercise Volume and Time Commitment. *PLoS One* **11**, e0154075 (2016).

80. Jamnick NA, Botella J, Pyne DB, Bishop DJ. Manipulating graded exercise test variables affects the validity of the lactate threshold and V˙ O2peak. *PLoS One* **13**, e0199794 (2018).

81. Christiansen D, MacInnis MJ, Zacharewicz E, Xu H, Frankish BP, Murphy RM. A fast, reliable and sample-sparing method to identify fibre types of single muscle fibres. *Scientific Reports* **9**, 6473 (2019).

82. Schaart G, Hesselink RP, Keizer HA, van Kranenburg G, Drost MR, Hesselink MK. A modified PAS stain combined with immunofluorescence for quantitative analyses of glycogen in muscle sections. *Histochem Cell Biol* **122**, 161-169 (2004).

83. Bloemberg D, Quadrilatero J. Rapid Determination of Myosin Heavy Chain Expression in Rat, Mouse, and Human Skeletal Muscle Using Multicolor Immunofluorescence Analysis. *PLOS ONE* **7**, e35273 (2012).

84. Li J, *et al*. TMTpro reagents: a set of isobaric labeling mass tags enables simultaneous proteome-wide measurements across 16 samples. *Nature Methods* **17**, 399-404 (2020).

85. Brenes A, Hukelmann J, Bensaddek D, Lamond AI. Multibatch TMT Reveals False Positives, Batch Effects and Missing Values. *Mol Cell Proteomics* **18**, 1967-1980 (2019).

86. Robinson MD, Oshlack A. A scaling normalization method for differential expression analysis of RNA-seq data. *Genome Biology* **11**, R25 (2010).

87. Johnson WE, Li C, Rabinovic A. Adjusting batch effects in microarray expression data using empirical Bayes methods. *Biostatistics* **8**, 118-127 (2007).

88. Plubell DL, *et al*. Extended Multiplexing of Tandem Mass Tags (TMT) Labeling Reveals Age and High Fat Diet Specific Proteome Changes in Mouse Epididymal Adipose Tissue. *Mol Cell Proteomics* **16**, 873-890 (2017).

89. Liu H, Sadygov RG, Yates JR, 3rd. A model for random sampling and estimation of relative protein abundance in shotgun proteomics. *Analytical chemistry* **76**, 4193-4201 (2004).

90. Ritchie ME, *et al.* limma powers differential expression analyses for RNA-sequencing and microarray studies. *Nucleic acids research* **43**, e47 (2015).

91. Rath S, *et al.* MitoCarta3.0: an updated mitochondrial proteome now with sub-organelle localization and pathway annotations. *Nucleic acids research*, (2020).

92. Huang DW, Sherman BT, Lempicki RA. Systematic and integrative analysis of large gene lists using DAVID bioinformatics resources. *Nature protocols* **4**, 44-57 (2009).

Figure 1 Legend

a) Workflow for characterisation of pooled human skeletal muscle fibres. Single fibres from human biopsy muscle samples were taken and fibre typing was confirmed through dot blotting. After optimisation, 6 single fibres were pooled and proteins were extracted using a S-Trap™ sample processing spin column before being labelled with a TMT labelling protocol. LC-MS3 was subsequently performed to quantify proteins for data analysis.

b) Percentage of proteins identified within the samples in comparison with the human genome. The bars display the percentage of proteins identified in the particular gene ontology cellular compartment (GOCC) group based on i) the average number of proteins identified within individual pooled samples (pink), ii) proteins identified within the entire dataset of high confidence proteins (orange) and iii) known annotated proteins in the human genome, not detected in entire single fibre dataset (grey). Identification of GOCC terms was completed using the DAVID functional annotation tool.

c) A Venn diagram displaying the number of proteins identified in the current study alongside the results of the two published single-fibre papers published to date. Due to differences in experimental design, and to make valid comparisons, the data of Murgia et al. (2017) were filtered for young participants with less than 30% missing values and the data of Deshmukh et al. (2021) were filtered for proteins with less than 30% missing values.

d) Proteins identified by all three single fibre studies in Figure 1c underwent GOCC analysis. The top 5 terms of the 844 proteins identified in the intersect of the proteins identified by Deshmukh et al., Reisman et al. and Murgia et al. are presented. The top GOCC terms and corresponding $\log_{10}$ P value were identified using the DAVID software [92] and computed by a Fisher's Exact Test.

e) Multidimensional Scaling (MDS) Plot used to show the distances among fibre types for PRE exercise type I (blue) and type II (red) samples.

f) Volcano plot illustrating the fold change distribution and significance of proteins in the PRE samples between type I and type II fibres. Points were coloured if they had a p value < 0.05 and log2 Fold Difference of > 0.2 (higher in Type II fibres) or < -0.2 (higher in Type I fibres). Points were labelled based on whether they were identified as differentially expressed uniquely within our study (compared with the differentially expressed proteins identified in Deshmukh et al. 2021 and Murgia et al. 2017).

g) Heatmap displaying z-score values of differentially expressed proteins when comparing type II to type I fibre pools within the PRE samples. Samples predominately cluster together by fibre type I (blue) or type II (red).

Figure 2 Legend

a) A Venn diagram displaying the number of mitochondrial proteins annotated according to the mitochondrial protein database Mitocarta 3.0 [91] in the current study, alongside two published human single-fibre datasets (Deshmukh et al. 2021 and Murgia et al. 2017). Only proteins with less than 30% missing data pre-intervention were annotated to Mitocarta 3.0.

b) Top gene ontology biological processes (GOBPs) in which the identified mitochondrial proteins common to all three studies illustrated in Fig 2a are mainly involved. The bars represent $Log_{10}P$ values, where *P* represents the significance of each GOBP enriched by the mitochondrial proteins. The *P*-value was computed using DAVID software [92].

c) Illustration of mitochondrial proteins that were differentially expressed between type I and type II fibres in the PRE samples following standard normalisation (Upper panel) and (Lower Panel) proteins that were identified as differentially expressed when the abundance of individual mitochondrial proteins was expressed relative to the total mitochondrial protein abundance of each fibre type (i.e., mitochondria-corrected relative abundance) [8]. Proteins that are no longer differentially expressed following mitochondrial normalisation are shaded. Proteins were labelled as mitochondrial according to Mitocarta 3.0 [91].

d) Comparison of Mean Mitochondrial Protein Expression in PRE exercise samples for type I (blue) and type II fibres (red).

Figure 3 Legend

a) The 8-week exercise training regime and methodology. Skeletal muscle biopsies were taken before week 1 and after week 8. Participants were randomly allocated into either the moderate-intensity continuous training (MICT) or sprint interval training (SIT) group. Grey bars indicate the number of training sessions per week. Following biopsies, muscle fibres were isolated into a single fibres. Single fibre lysates were fibre typed according to dot blotting and subsequently pooled by fibre type (six fibres). Samples then underwent LC-MS3 analysis.

b) Bar graphs displaying fold differences between the moderate-intensity continuous training (MICT) and sprint interval training (SIT) for exercise intensity (%W_{max}) and total training volume (J). Also shown are bar graphs displaying the change in blood lactate concentration (mmol•L^{-1}) and hydrogen ion (H^+) concentration (mol•L^{-1}) from pre to post exercise following the first moderate-intensity continuous exercise (MICT) and the first sprint interval exercise (SIT) session. Mean ± standard deviation ; * adjusted P value < 0.05.

c) *Histochemistry* – A representative example of the effects of a single session of exercise on fibre-type specific glycogen depletion patterns in cross-sections of human vastus lateralis muscle samples collected before and after either moderate-intensity continuous exercise (MICT) or sprint interval exercise (SIT). The top panels display immunofluorescent fibre-type staining for myosin heavy chain content, with type I muscle fibres (MHC7) identified as blue and type II fibres (MHC2) identified as green. The bottom panels display serial sections that have been stained for glycogen (periodic acid-Schiff staining). Bars = 200 µm.

d) Illustration of the proposed hierarchal recruitment pattern of type I and IIa skeletal muscle fibres in relation to exercise intensity. Moderate-intensity continuous exercise (MICT) is indicated in purple and sprint interval exercise (SIT) in green, with type I fibres and type II fibres in blue and red, respectively.

Figure 4 Legend

a) Methodology used to compare Reisman et al. and Deskhmukh et al. 2021 for MICT type I PRE vs POST samples. The methodology shows that proteins were removed from the raw data if there was more than 70% missing data across the total matrix;

this was followed by imputation with KNN nearest neighbor averaging with differential expression comparisons.

b) - d) Volcano plots illustrating the fold-change distribution of proteins within Type I fibres following MICT for Reisman et al. (panel B) and Deshmukh et al (panel C and D). Proteins are coloured in teal based if the proteins were differentially expressed with an unadjusted p-value of < 0.05 (panel b and c) or significant with a fusion factor of < 0.05 (Xiao et al., 2014) (panel d); when the values in b) and c) were adjusted using the Benjamini–Hochberg method for multiple hypothesis testing, none of these proteins remained significant.

Figure 5 Legend

a) Volcano plot illustrating the distribution of proteins that were differentially expressed between type I and II fibres in the POST MICT samples. Points were labelled based on whether they were identified as differentially expressed, according to adjusted P values from the *limma* analysis.

b) Volcano plot illustrating the distribution of proteins that were differentially expressed between type I and II fibres in the POST SIT samples. Points were labelled based on whether they were identified as differentially expressed, according to adjusted P values from the *limma* analysis.

c) Venn Diagrams displaying the number of proteins identified as higher in type I or type II fibres for both exercise types, with the proteins that appear in both datasets seen in the overlap. Individual proteins are listed in supplemental Table 5, Tab 3.

d) Venn Diagram displaying the number of proteins that were differentially expressed between type I and type II fibres in the PRE samples (n=16 participants), compared with the number of differentially expressed proteins between type I and type II fibres in the POST MICT (n = 8) and SIT samples (n=8).

e) *EnrichPlot* dot plot results of protein expression in type I vs type II fibres for the POST MICT and SIT samples. Pathway terms were identified using WikiPathways. The top 15 terms, according to adjusted P-values, are displayed. Red dots identify pathway terms found higher in type II fibres, while blue dots indicate pathway terms found higher in type I fibres. The saturation of each colour is proportional to the average log2 fold difference for each exercise and fibre group. The size of each dot indicates how many proteins correspond to each pathway term. For all proteins, the

corresponding log_2 fold change and P-values from the differential expression analysis were used. All terms identified can be found in supplemental Table 5, Tab 5.

f) *ClusterProfiler* network plot using differentially expressed (adjusted P value < 0.05) terms. Pathway terms were identified using WikiPathways. Colours indicate in which exercise and fibre group the proteins in that WikiPathway term were found. The size of each circle indicates how many proteins corresponded to each term. The displayed terms were manually selected for readability of the figure. All terms identified can be found in supplemental Table 5, Tab 6.

Figure 6 Legend

a) Representative images of skeletal muscle samples analysed using transmission electron microscopy (TEM) pre- and post-training for participants who performed either moderate-intensity continuous training (MICT) or sprint interval training (SIT). Note the difference in the abundance of mitochondria post MICT. Bars = 0.5 µm

b) Violin plots of change (Δ) in mitochondrial volume density (% $Mito_{VD}$) from pre- to post-training following MICT (purple) and SIT (green).

c) Violin plots of change (Δ) in citrate synthase activity (CS; $mol.h^{-1}.kg\ protein^{-1}$) from pre- to post-training following MICT (purple) and SIT (green).

d) Scaled profile plots showing the relative abundance of mitochondrial proteins (grey) pre- and post-exercise in the MICT (purple) and SIT (green) groups for each fibre type, and the mean relative abundance (black) of the proteins in each group. Data are shown as Δ mean z-score. * indicates P values for significance (*: P <= 0.01, **: P <= 0.001, ***: P <= 0.0001, ****: P <= 0.00001) by paired t-test from pre- to post-training.

Figure 7 Legend

a) Scaled profile plots with the application of mitochondrial normalisation showing changes in the relative abundance of mitochondrial proteins (grey) pre- and post-training in the moderate-intensity continuous training (MICT) and sprint interval training (SIT) groups for each fibre type. The mean of each group is indicated by the black line. Data is shown as Δ mean z-score.

b) Scaled profile plots with the application of mitochondrial normalisation showing changes in the relative abundance of the subunits in each of the oxidative phosphorylation (OXPHOS) complexes (CI to CV), as well as the mitochondrial ribosome, in type I and type II fibre types in response to both types of training (MICT and SIT). The mean of each group (all proteins identified in each pathway using MitoCarta 3.0) is indicated by the black line. Data is shown as Δ mean z-score.
* indicate P value for significance (**: P ≤ 0.001) based on a paired t-test of the pre- to post-training values.

c) Heatmap displaying z-score values of protein subunits of the OXPHOS complexes, as well as the mitochondrial ribosome, in each of the two training groups (MICT and SIT), in type I and type II fibre types pre- and post-training, with the application of mitochondrial normalisation.

d) Scaled profile plots with the application of mitochondrial normalisation showing changes in the relative abundance of proteins involved in Fatty Acid Oxidation, the tricarboxylic acid cycle, and mitochondrial dynamics (all proteins identified in pathway using MitoCarta 3.0) in type I and type II fibre types in response to both types of training (MICT and SIT). The mean of each group is indicated by the black line. Data are shown as Δ mean z-score. * indicate P value for significance (*: P ≤ 0.01, **: P ≤ 0.001) based on a paired t-test of the pre- to post-training values.

Supplemental Figure 1 Legend

a) Heatmap displaying z-score values of protein subunits of the OXPHOS complexes, as well as the mitochondrial ribosome, in each of the two training groups, moderate-intensity continuous training (MICT) or sprint interval training (SIT), in type I and type II fibre types pre- and post-training, without the application of mitochondrial normalisation.

b) Scaled profile plots without the application of mitochondrial normalisation showing changes in the relative abundance of the subunits in each of the oxidative phosphorylation (OXPHOS) complexes (CI to CV), as well as the mitochondrial ribosome, in type I and type II fibre types in response to both types of training (MICT and SIT). The mean of each group (all proteins identified in each pathway using MitoCarta 3.0) is indicated by the black line. Data are shown as Δ mean z-score. *

indicate P value for significance (*: P ≤ 0.01, **: P ≤ 0.001, ***: P ≤ 0.0001, ****: P ≤ 0.00001) based on a paired t-test of the pre- to post-training values.

c) Scaled profile plots without the application of mitochondrial normalisation showing changes in the relative abundance of proteins involved in fatty acid 0xidation, the tricarboxylic acid cycle, and mitochondrial dynamics (all proteins identified in pathway using MitoCarta 3.0) in type I and type II fibre types in response to both types of training (MICT and SIT). The mean of each group is indicated by the black line. Data are shown as Δ mean z-score. * indicate P value for significance (*: P ≤ 0.01, **: P ≤ 0.001, ***: P ≤ 0.0001, ****: P ≤ 0.00001) based on a paired t-test of the pre- to post-training values.

Supplementary Figure 2 Legend

a) The number of proteins quantified in the training study dataset by our proteomic workflow in all pooled single-fibre samples. Samples are arranged according to TMT batches (A-H). Samples are labelled according to participant ID (Z to A), training type (S for SIT or M for MICT), biopsy time (pre or post), and fibre type (I or II))

b) Reproducibility of protein intensities (intensity-based absolute quantification; IBAQ) for replicates of type I skeletal muscle fibre samples. Core mitochondrial proteins (OXPHOS – NDUFA8, SDHA, URCRC2, COX5B, ATP5B, IDH3B and CKM) are highlighted in yellow, in addition to sarcomeric proteins (MYH 7 (blue), ACTA1 (orange)).

c) Reproducibility of protein intensities (intensity-based absolute quantification; IBAQ) for replicates of type II skeletal muscle fibre samples. Core mitochondrial proteins (OXPHOS – NDUFA8, SDHA, URCRC2, COX5B, ATP5B, IDH3B and CKM) are highlighted in yellow, in addition to MYH2 (green).

d) Relative abundance of myosin heavy chains (MYH) in type I samples pooled by dot blotting, according to the percentage of the MYH7 (blue = type I), MYH2 (red = type-IIa) MYH1 (brown = type-IIx), and MYH4 (purple = type IIb) protein isoforms detected.

e) Relative abundance of myosin heavy chains (MYH) in type II samples pooled by dot blotting, according to the percentage of the MYH7 (blue = type I), MYH2 (red = type-IIa) MYH1 (brown = type-IIx), and MYH4 (purple = type IIb) protein isoforms detected.

f) Study recruitment flow chart and final group sizes used within the study.

g) Hierarchical visualisation of the statistical comparisons performed in this study.

h) Depth of coverage in pooled single fibre samples for the number of proteins and peptides identified.

i) Fibre Typing by dot blotting. This example shows membrane images for the identification of fibre types in a single participant. Type I fibres were identified via the presence of MHCI (left panel) and type II fibres were identified via the presence of MHCIIa (right panel).

Description of Additional Supplementary Files

File name: Supplementary Table 1

Description: Participant characteristics, Raw intensities for all proteomic data, and log intensities for all identified proteins in all samples following the normalisation described in the methods. Data also includes gene ontology cellular compartment (GOCC) analysis for pooled single fibre analysis for percentage of cellular compartment identified (shown in Figure 1b) and the top 5 GOCC and corresponding $\log_{10}$ P value identified using the DAVID software for proteins identified by key single fibre proteomic studies (shown in Figure 1c). Further analysis includes the protein lists presented in the Venn diagram of Figure 1c for identified proteins within the current study, along with the studies of Deshmukh et al. and Murgia et al. (Tab 5), along with the top GOCC terms for the common proteins identified in all 3 studies (Fig 1d, Tab 6). Statistical analysis is lastly presented via logged intensities of proteins within the PRE type I and type II fibre samples. The table also displays calculations completed to calculate the 'Fusion Factor' used in Deshmukh et al. (2021) and the corresponding significance. Further detail is provided in the legend tab of the linked Excel file.

File name: Supplementary Table 2

Description: The list of mitochondrial proteins (according to Mitocarta 3.0) in common to all previous single fibre human studies pre intervention. Further analysis is presented in the table output by the DAVID software to identify top gene ontology biological processes (GOBP) groups of the mitochondrial proteins identified in over 70% of the total sample in all three studies listed (Deshmukh et al., Murgia et al., and the current study). Further analysis is presented with the average of all mitochondrial proteins in each individual. The mean of averages were calculated and compared between PRE training type I fibres and type II fibres. Mitochondrial protein expression (MPE) calculation is subsequently presented for identified mitochondrial proteins within the study in each comparison. Data normalised for mitochondrial content for identified mitochondrial proteins within the study for the PRE type I vs II comparison and presented in the volcano plots (Figure 2f). Further detail provided in the legend tab of the linked Excel file.

File name: Supplementary Table 3

Description: Fold Difference from Pre to Post exercise for blood concentration of H^+ and lactate results.

File name: Supplementary Table 4

Description: The normalised Data (Log2) with *limma* and Fusion Factor calculations for MICT Type I and Type II - PRE vs POST. In addition, Normalised Data (Log_2 with *limma* and Fusion Factor Calculations for SIT type I & type II - PRE vs POST. Proteins identified in type I vs type II fibres POST MICT and corresponding GO Biological Processes results. Parallel analysis is presented for POST SIT. Further detail is provided in the legend tab of the linked Excel file.

File name: Supplementary Table 5

Description: Log intensities for type I versus type II fibres in POST MICT and SIT samples following normalisation. GO Enrichment (Biological Processes) completed with DAVID on the common and unique MICT and SIT proteins identified when comparing Post I vs II samples. Further corresponding GOBP analysis is also made proteins identified as differentially expressed between type I and II fibres in the PRE samples. Further enrichment analysis is undertaken via WikiPathways enrichment analysis and Network analysis of differences in protein abundance between type I & type II fibres in the POST samples for MICT & SIT (analysed separately), using enrichplot & clusterprofiler on the *limma* results displayed in Tab 1 and 2 of this file. Further detail provided in the legend tab of the linked Excel file.

File name: Supplementary Table 6

Description: Differences from Pre to Post training for Mitochondria Volume Density (%) and Citrate Synthase activity ($mol \cdot h^{-1} \cdot kg\ protein^{-1}$) for MICT & SIT. Analysis presented for scaled intensities (z-scores) and means for known mitochondrial proteins for all samples following standard normalisation. Scaled means for each complex in each sample group are also presented in addition to the mean change for each comparison of training and fibre type. Further detail is provided in the legend tab of the linked Excel file.

File name: Supplementary Table 7

Description: Scaled intensities and means for known mitochondrial proteins for all samples following mitochondrial normalisation. Protein functional classes and metabolic pathways presented with the scaled means (z-scores) for each functional group (defined by MitoCarta

3.0) in each sample group in addition to the mean change for each comparison of training and fibre type with mitochondrial normalisation applied. Further detail provided in the legend tab of the linked Excel file.

File name: Supplementary Table 8

Description: Protein functional classes and metabolic pathways presented with the scaled means (z-scores) for each functional group (defined by MitoCarta 3.0) in each sample group in addition to the mean change for each comparison of training and fibre type. Further detail is provided in the legend tab of the linked Excel file.

File name: Supplementary Table 9

Description: The number of proteins quantified in the training study dataset by our proteomic workflow in all pooled single-fibre samples. Raw TMT Batch ID is presented and arranged according to TMT batches (A-H). Samples are labelled according to participant ID (Z-C), training type (S for SIT or M for MICT), training time (pre or post) and fibre type (I or II). In addition, reliability between replicates is presented - List of Intensity reported by intensity-based absolute quantification (IBAQ) for replicates and corresponding gene names of pooled type I fibres (n = 6 fibres) and type II fibres. Furthermore, the relative TMT intensity and percentage abundance of myosin heavy chains (MYH) for type I and type II samples pooled by dot blotting is presented.

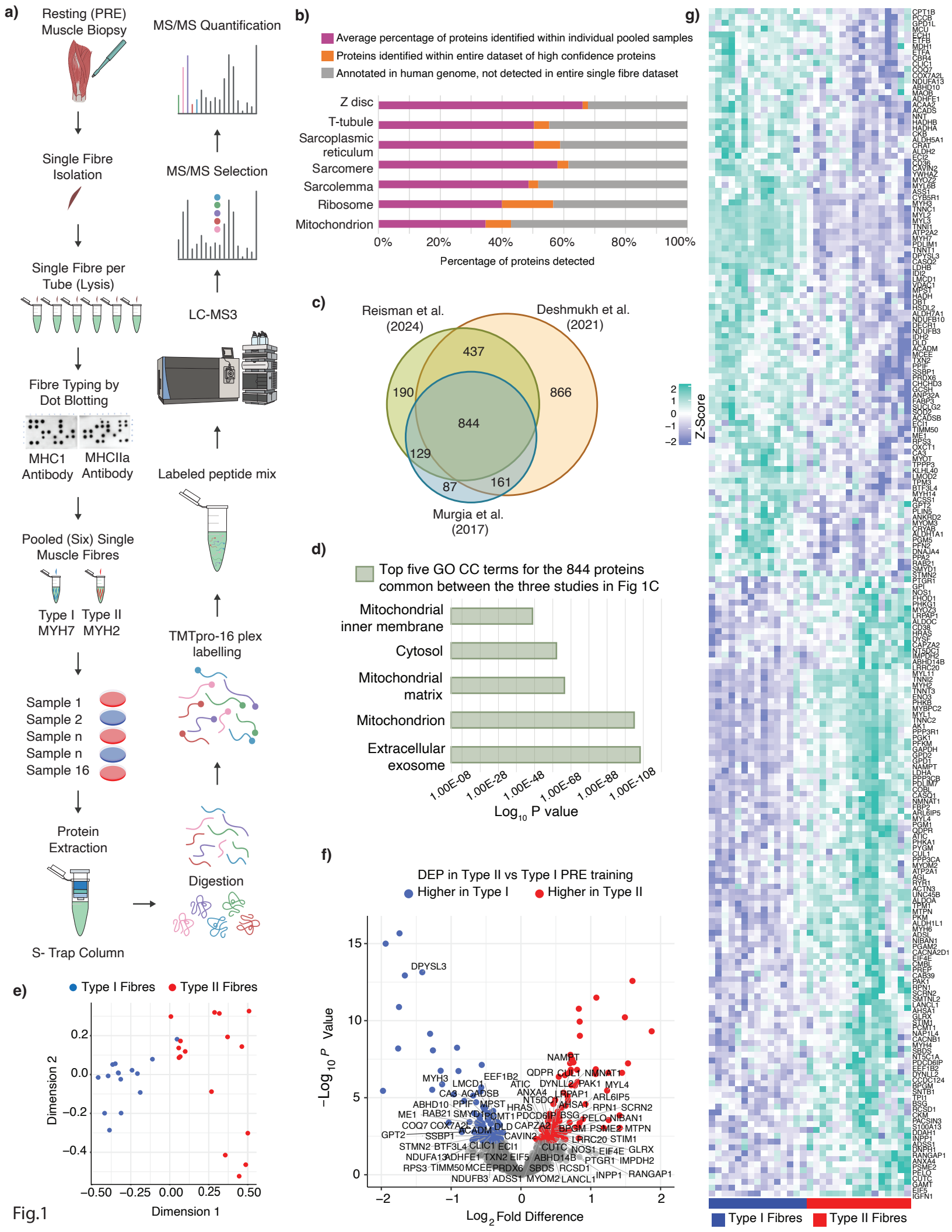
a)
Resting (PRE) Muscle Biopsy
Single Fibre Isolation
Single Fibre per Tube (Lysis)
Fibre Typing by Dot Blotting
MHC1 Antibody
MHCIIa Antibody
Pooled (Six) Single Muscle Fibres
Type I MYH7
Type II MYH2
Sample 1
Sample 2
Sample n
Sample n
Sample 16
Protein Extraction
S- Trap Column
Digestion
TMTpro-16 plex labelling
Labeled peptide mix
LC-MS3
MS/MS Selection
MS/MS Quantification
b)
Average percentage of proteins identified within individual pooled samples
Proteins identified within entire dataset of high confidence proteins
Annotated in human genome, not detected in entire single fibre dataset
Z disc
T-tubule
Sarcoplasmic reticulum
Sarcomere
Sarcolemma
Ribosome
Mitochondrion
0%
20%
40%
60%
80%
100%
Percentage of proteins detected
c)
Reisman et al. (2024)
Deshmukh et al. (2021)
Murgia et al. (2017)
437
190
866
844
129
87
161
d)
Top five GO CC terms for the 844 proteins common between the three studies in Fig 1C
Mitochondrial inner membrane
Cytosol
Mitochondrial matrix
Mitochondrion
Extracellular exosome
1.00E-08
1.00E-28
1.00E-48
1.00E-68
1.00E-88
1.00E-108
Log10 P value
e)
Type I Fibres
Type II Fibres
Dimension 2
Dimension 1
f)
DEP in Type II vs Type I PRE training
Higher in Type I
Higher in Type II
−Log10 P Value
Log2 Fold Difference
DPYSL3
NAMPT
g)
Z-Score
Type I Fibres
Type II Fibres

Fig.1

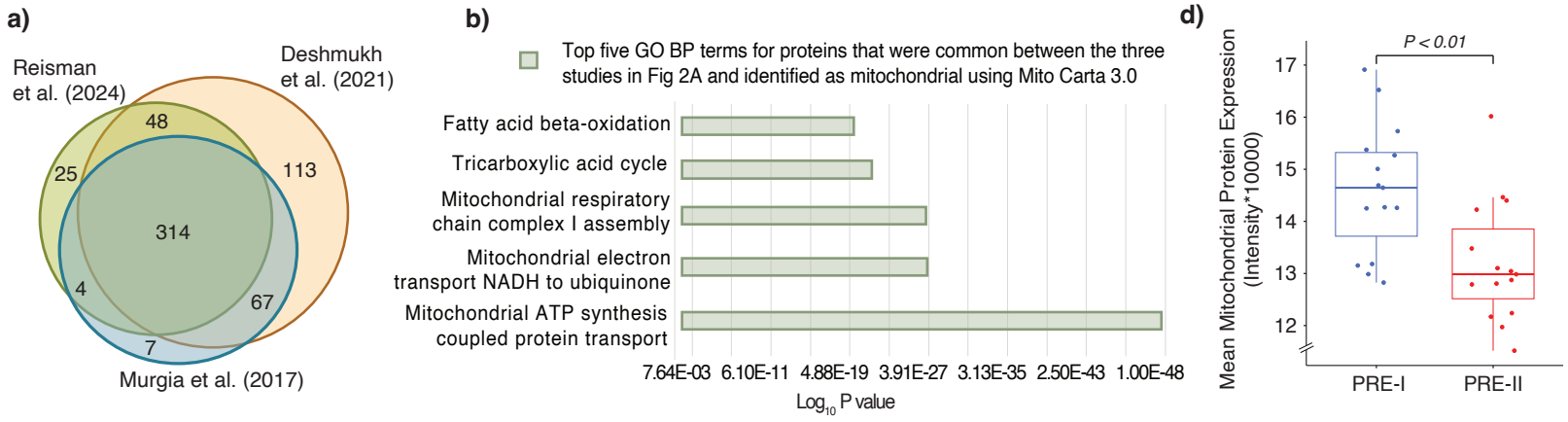

c)

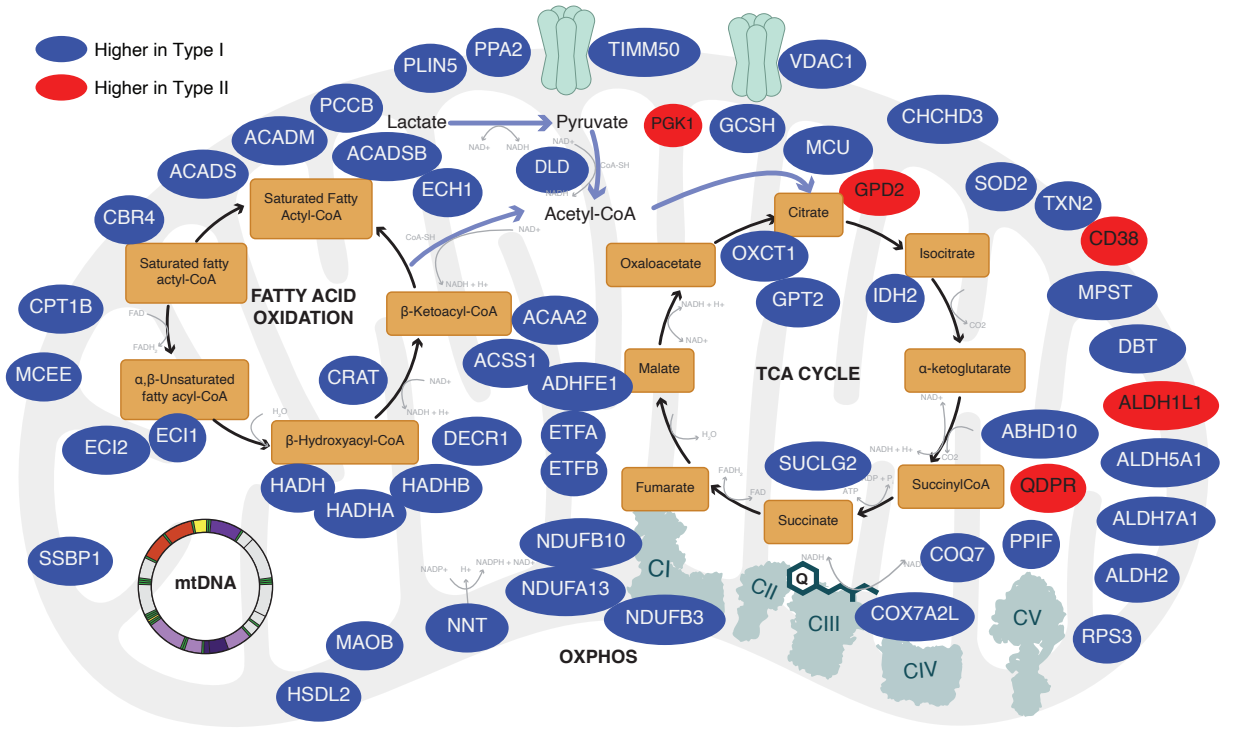

Differentially Expressed Mitochondrial Proteins in Non Mitochondria-Corrected Data

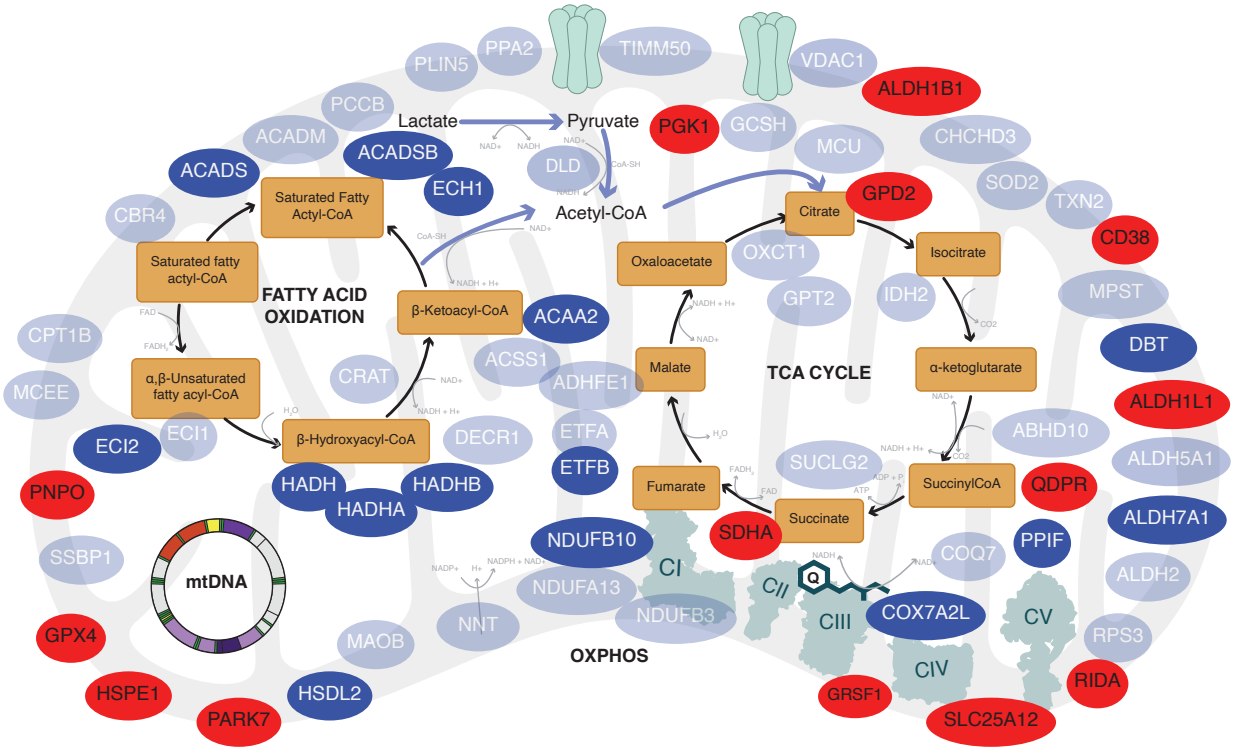

Differentially Expressed Mitochondrial Proteins in Mitochondria-Corrected Data

Fig.2

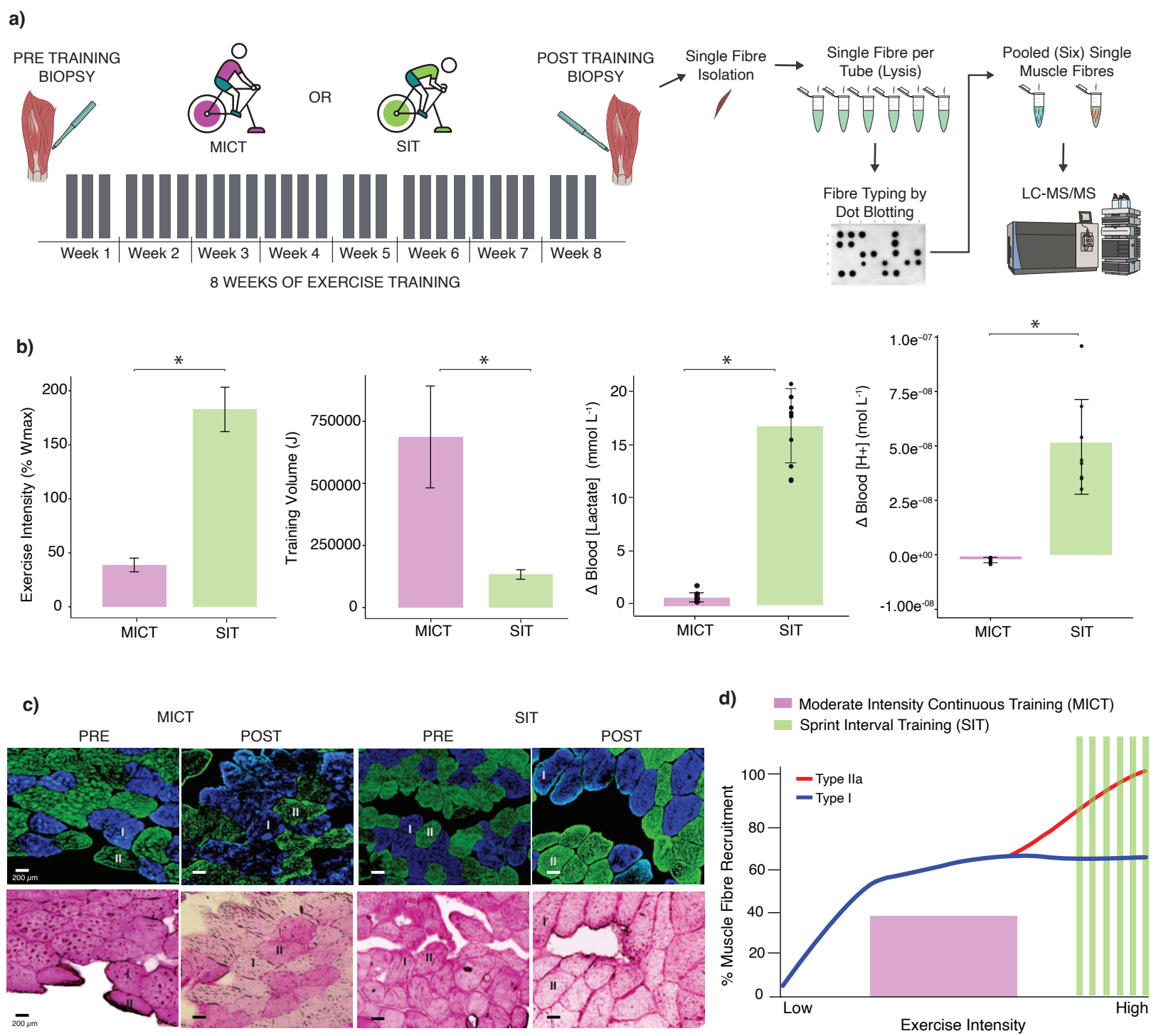
a)
PRE TRAINING BIOPSY
MICT
OR
SIT
POST TRAINING BIOPSY
Single Fibre Isolation
Single Fibre per Tube (Lysis)
Pooled (Six) Single Muscle Fibres
Fibre Typing by Dot Blotting
LC-MS/MS
Week 1
Week 2
Week 3
Week 4
Week 5
Week 6
Week 7
Week 8
8 WEEKS OF EXERCISE TRAINING
b)
Exercise Intensity (% Wmax)
Training Volume (J)
Δ Blood [Lactate] (mmol L⁻¹)
Δ Blood [H+] (mol L⁻¹)
MICT
SIT
c)
MICT
SIT
PRE
POST
200 μm
d)
Moderate Intensity Continuous Training (MICT)
Sprint Interval Training (SIT)
Type IIa
Type I
% Muscle Fibre Recruitment
Low
High
Exercise Intensity

Fig.3

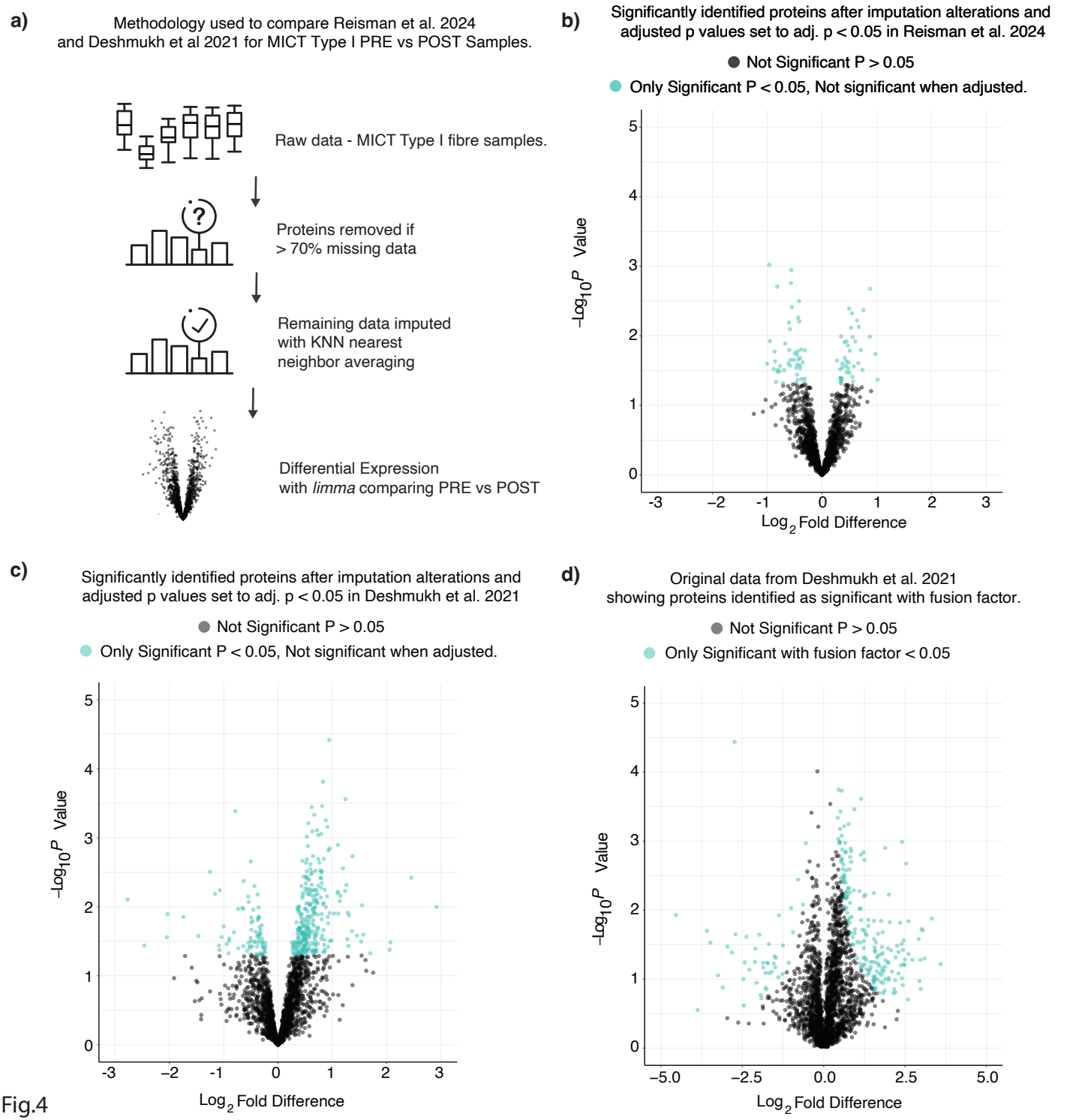
a)
Methodology used to compare Reisman et al. 2024
and Deshmukh et al 2021 for MICT Type I PRE vs POST Samples.
Raw data - MICT Type I fibre samples.
Proteins removed if
> 70% missing data
Remaining data imputed
with KNN nearest
neighbor averaging
Differential Expression
with limma comparing PRE vs POST
b)
Significantly identified proteins after imputation alterations and
adjusted p values set to adj. p < 0.05 in Reisman et al. 2024
Not Significant P > 0.05
Only Significant P < 0.05, Not significant when adjusted.
−Log10P Value
Log2 Fold Difference
c)
Significantly identified proteins after imputation alterations and
adjusted p values set to adj. p < 0.05 in Deshmukh et al. 2021
Not Significant P > 0.05
Only Significant P < 0.05, Not significant when adjusted.
−Log10P Value
Log2 Fold Difference
d)
Original data from Deshmukh et al. 2021
showing proteins identified as significant with fusion factor.
Not Significant P > 0.05
Only Significant with fusion factor < 0.05
−Log10P Value
Log2 Fold Difference

Fig.4

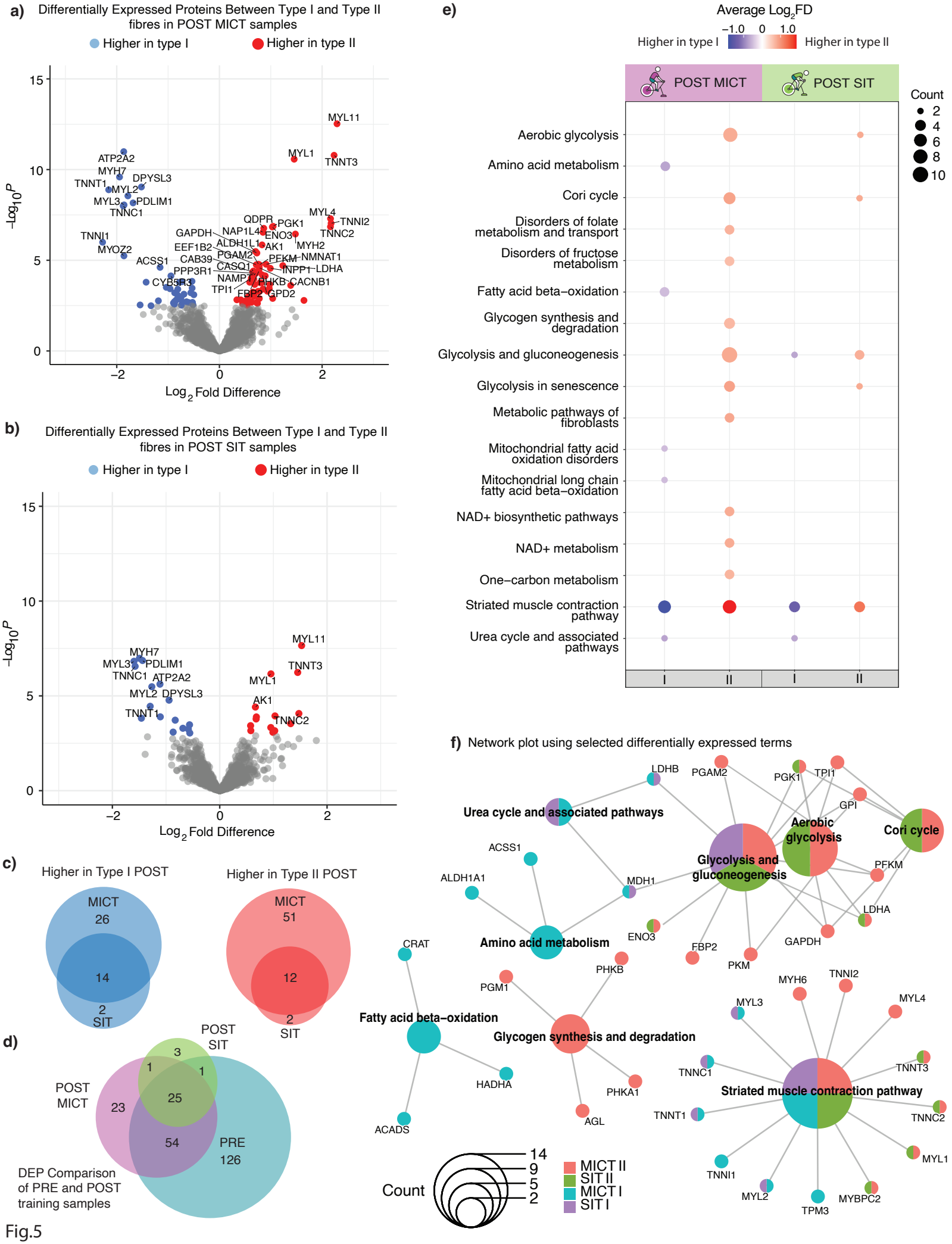
a)
Differentially Expressed Proteins Between Type I and Type II fibres in POST MICT samples
Higher in type I
Higher in type II
−Log10P
Log2 Fold Difference
MYL11
MYL1
TNNT3
ATP2A2
MYH7
DPYSL3
TNNT1
MYL2
MYL3
PDLIM1
TNNC1
MYL4
TNNI2
QDPR
PGK1
GAPDH
NAP1L4
ENO3
TNNC2
TNNI1
EEF1B2
ALDH1L1
AK1
MYH2
MYOZ2
PGAM2
ACSS1
CAB39
PFKM
NMNAT1
CASQ1
INPP1
LDHA
PPP3R1
NAMPT
PHKB
CACNB1
CYB5R3
TPI1
FBP2
GPD2
b)
Differentially Expressed Proteins Between Type I and Type II fibres in POST SIT samples
Higher in type I
Higher in type II
−Log10P
Log2 Fold Difference
MYL11
MYH7
MYL3
PDLIM1
TNNC1
ATP2A2
TNNT3
MYL1
MYL2
DPYSL3
AK1
TNNT1
TNNC2
c)
Higher in Type I POST
MICT
26
14
2
SIT
Higher in Type II POST
MICT
51
12
2
SIT
d)
POST SIT
3
1
1
POST MICT
23
25
54
PRE
126
DEP Comparison of PRE and POST training samples
e)
Average Log2FD
−1.0
0
1.0
Higher in type I
Higher in type II
POST MICT
POST SIT
Count
2
4
6
8
10
Aerobic glycolysis
Amino acid metabolism
Cori cycle
Disorders of folate metabolism and transport
Disorders of fructose metabolism
Fatty acid beta−oxidation
Glycogen synthesis and degradation
Glycolysis and gluconeogenesis
Glycolysis in senescence
Metabolic pathways of fibroblasts
Mitochondrial fatty acid oxidation disorders
Mitochondrial long chain fatty acid beta−oxidation
NAD+ biosynthetic pathways
NAD+ metabolism
One−carbon metabolism
Striated muscle contraction pathway
Urea cycle and associated pathways
I
II
I
II
f)
Network plot using selected differentially expressed terms
LDHB
PGAM2
PGK1
TPI1
GPI
Urea cycle and associated pathways
Aerobic glycolysis
Cori cycle
ACSS1
Glycolysis and gluconeogenesis
PFKM
ALDH1A1
MDH1
LDHA
ENO3
GAPDH
CRAT
Amino acid metabolism
FBP2
PKM
PHKB
PGM1
MYH6
TNNI2
MYL3
MYL4
Fatty acid beta−oxidation
Glycogen synthesis and degradation
TNNC1
TNNT3
HADHA
PHKA1
Striated muscle contraction pathway
TNNT1
TNNC2
ACADS
AGL
MYL1
TNNI1
MYL2
TPM3
MYBPC2
Count
14
9
5
2
MICT II
SIT II
MICT I
SIT I

Fig.5

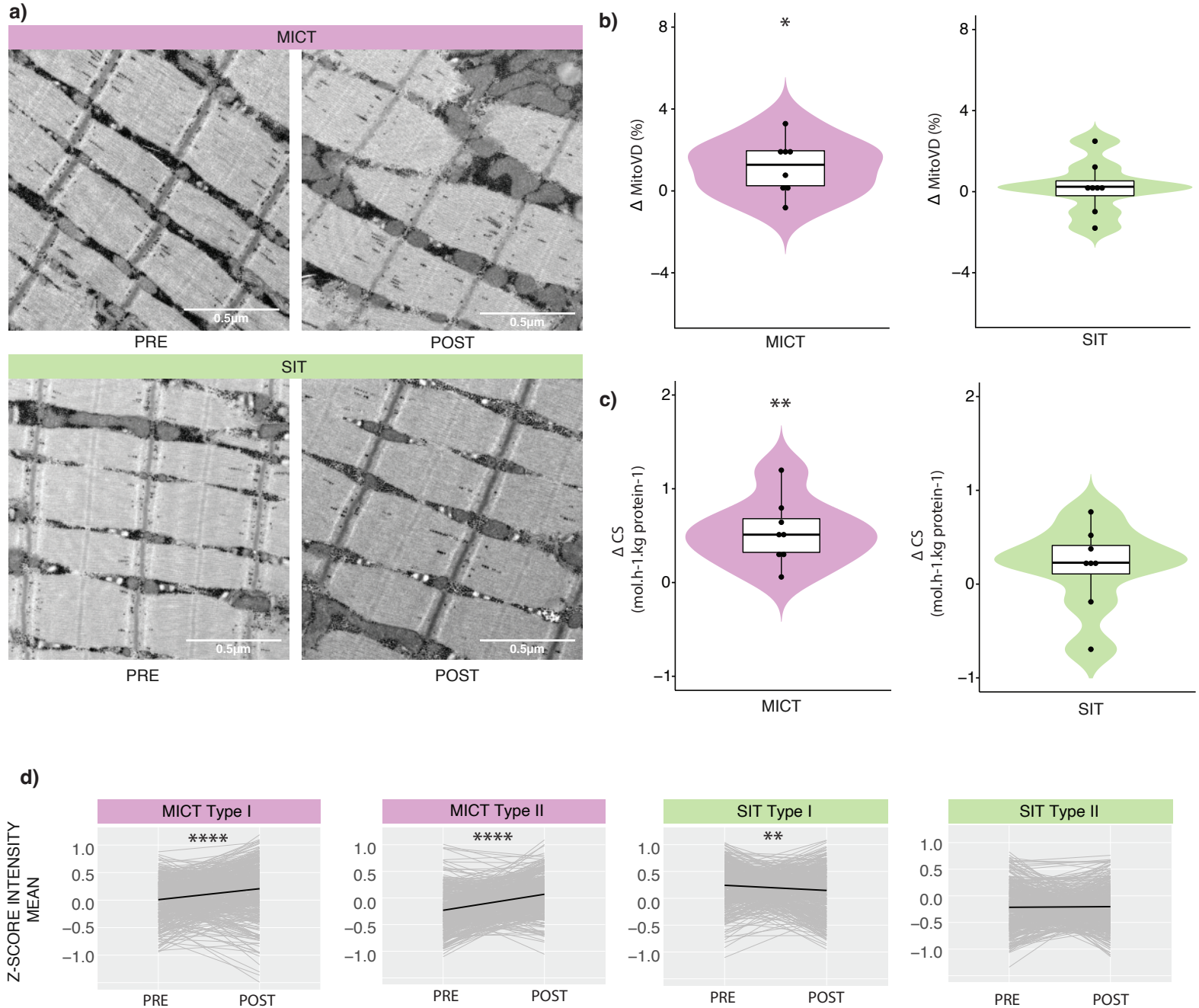
a)
MICT
0.5µm
0.5µm
PRE
POST
SIT
0.5µm
0.5µm
PRE
POST
b)
*
Δ MitoVD (%)
8
4
0
−4
MICT
SIT
c)
**
Δ CS (mol.h-1.kg protein-1)
2
1
0
−1
MICT
SIT
d)
MICT Type I
MICT Type II
SIT Type I
SIT Type II
****
****
**
Z-SCORE INTENSITY MEAN
1.0
0.5
0.0
−0.5
−1.0
PRE
POST

Fig.6

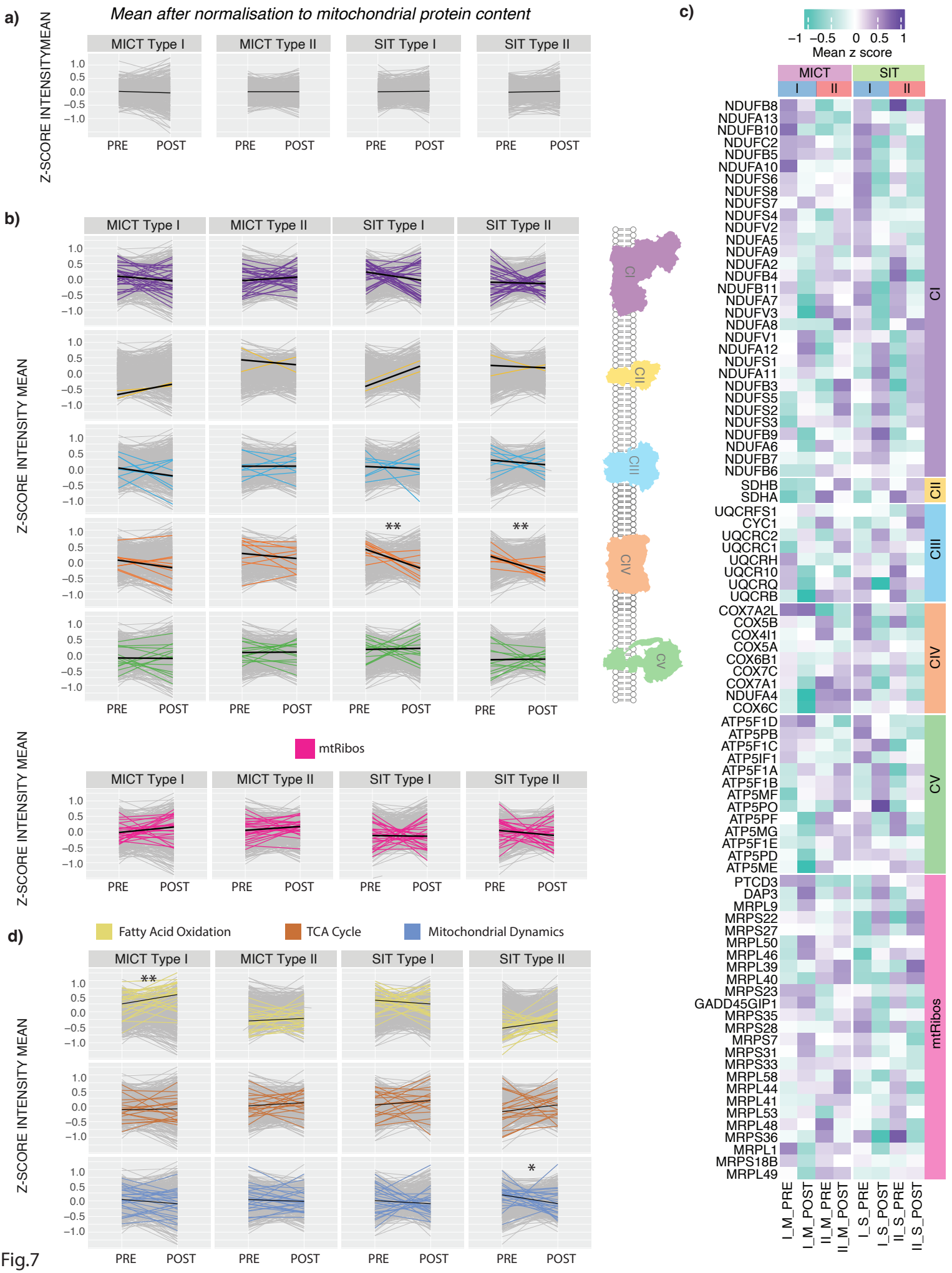
a)
Mean after normalisation to mitochondrial protein content
Z-SCORE INTENSITYMEAN
MICT Type I
MICT Type II
SIT Type I
SIT Type II
PRE
POST
b)
Z-SCORE INTENSITY MEAN
CI
CII
CIII
CIV
CV
mtRibos
c)
Mean z score
MICT
SIT
NDUFB8
NDUFA13
NDUFB10
NDUFC2
NDUFB5
NDUFA10
NDUFS6
NDUFS8
NDUFS7
NDUFS4
NDUFV2
NDUFA5
NDUFA9
NDUFA2
NDUFB4
NDUFB11
NDUFA7
NDUFV3
NDUFA8
NDUFV1
NDUFA12
NDUFS1
NDUFA11
NDUFB3
NDUFS5
NDUFS2
NDUFS3
NDUFB9
NDUFA6
NDUFB7
NDUFB6
SDHB
SDHA
UQCRFS1
CYC1
UQCRC2
UQCRC1
UQCRH
UQCR10
UQCRQ
UQCRB
COX7A2L
COX5B
COX4I1
COX5A
COX6B1
COX7C
COX7A1
NDUFA4
COX6C
ATP5F1D
ATP5PB
ATP5F1C
ATP5IF1
ATP5F1A
ATP5F1B
ATP5MF
ATP5PO
ATP5PF
ATP5MG
ATP5F1E
ATP5PD
ATP5ME
PTCD3
DAP3
MRPL9
MRPS22
MRPS27
MRPL50
MRPL46
MRPL39
MRPL40
MRPS23
GADD45GIP1
MRPS35
MRPS28
MRPS7
MRPS31
MRPS33
MRPL58
MRPL44
MRPL41
MRPL53
MRPL48
MRPS36
MRPL1
MRPS18B
MRPL49
I_M_PRE
I_M_POST
II_M_PRE
II_M_POST
I_S_PRE
I_S_POST
II_S_PRE
II_S_POST
d)
Fatty Acid Oxidation
TCA Cycle
Mitochondrial Dynamics

Fig.7

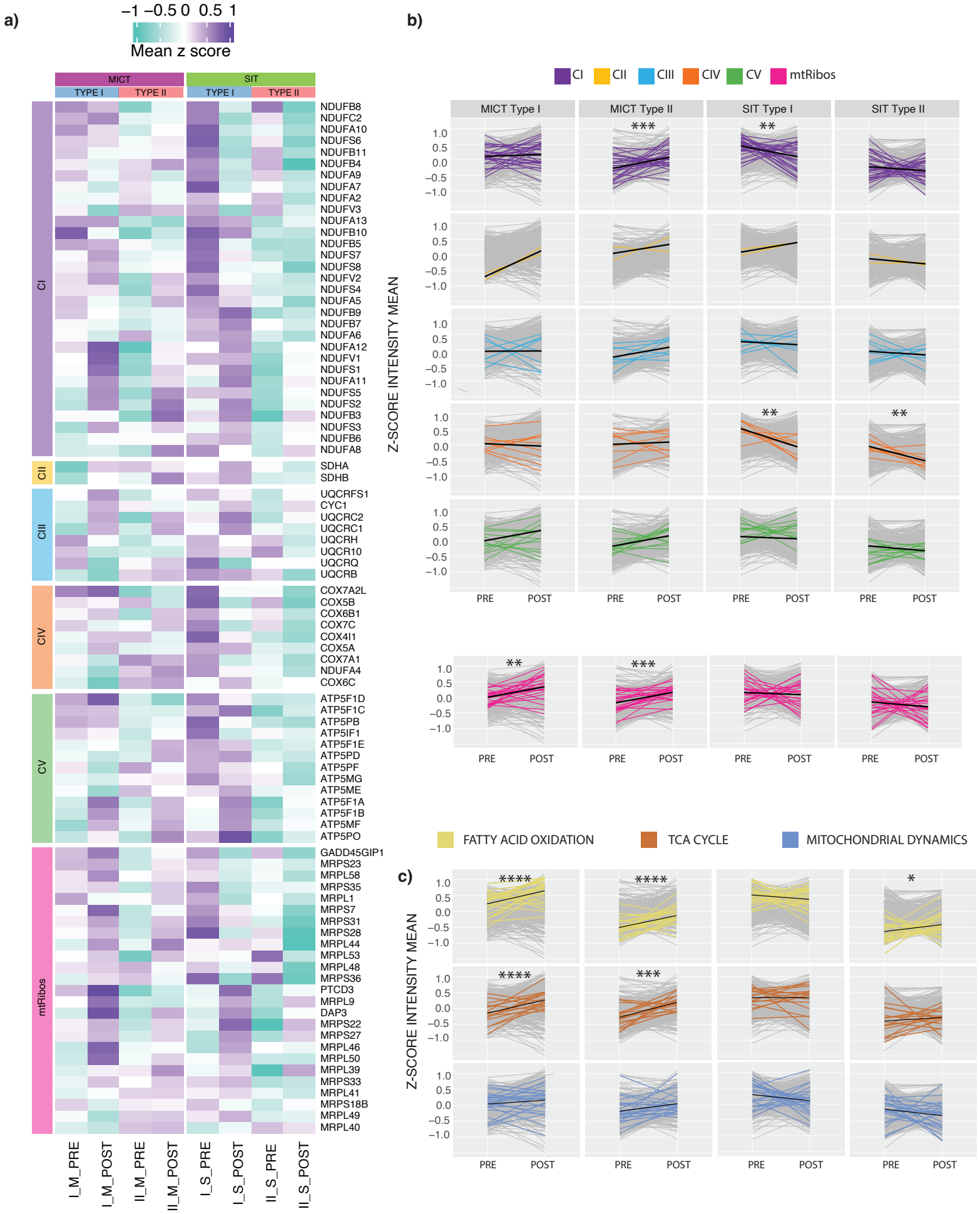
a)
−1 −0.5 0 0.5 1
Mean z score
MICT
SIT
TYPE I
TYPE II
CI
CII
CIII
CIV
CV
mtRibos
NDUFB8
NDUFC2
NDUFA10
NDUFS6
NDUFB11
NDUFB4
NDUFA9
NDUFA7
NDUFA2
NDUFV3
NDUFA13
NDUFB10
NDUFB5
NDUFS7
NDUFS8
NDUFV2
NDUFS4
NDUFA5
NDUFB9
NDUFB7
NDUFA6
NDUFA12
NDUFV1
NDUFS1
NDUFA11
NDUFS5
NDUFS2
NDUFB3
NDUFS3
NDUFB6
NDUFA8
SDHA
SDHB
UQCRFS1
CYC1
UQCRC2
UQCRC1
UQCRH
UQCR10
UQCRQ
UQCRB
COX7A2L
COX5B
COX6B1
COX7C
COX4I1
COX5A
COX7A1
NDUFA4
COX6C
ATP5F1D
ATP5F1C
ATP5PB
ATP5IF1
ATP5F1E
ATP5PD
ATP5PF
ATP5MG
ATP5ME
ATP5F1A
ATP5F1B
ATP5MF
ATP5PO
GADD45GIP1
MRPS23
MRPL58
MRPS35
MRPL1
MRPS7
MRPS31
MRPS28
MRPL44
MRPL53
MRPL48
MRPS36
PTCD3
MRPL9
DAP3
MRPS22
MRPS27
MRPL46
MRPL50
MRPL39
MRPS33
MRPL41
MRPS18B
MRPL49
MRPL40
I_M_PRE
I_M_POST
II_M_PRE
II_M_POST
I_S_PRE
I_S_POST
II_S_PRE
II_S_POST
b)
CI
CII
CIII
CIV
CV
mtRibos
MICT Type I
MICT Type II
SIT Type I
SIT Type II
Z-SCORE INTENSITY MEAN
1.0
0.5
0.0
−0.5
−1.0
***
**
PRE
POST
FATTY ACID OXIDATION
TCA CYCLE
MITOCHONDRIAL DYNAMICS
c)
****
***
*

Supp Fig.1

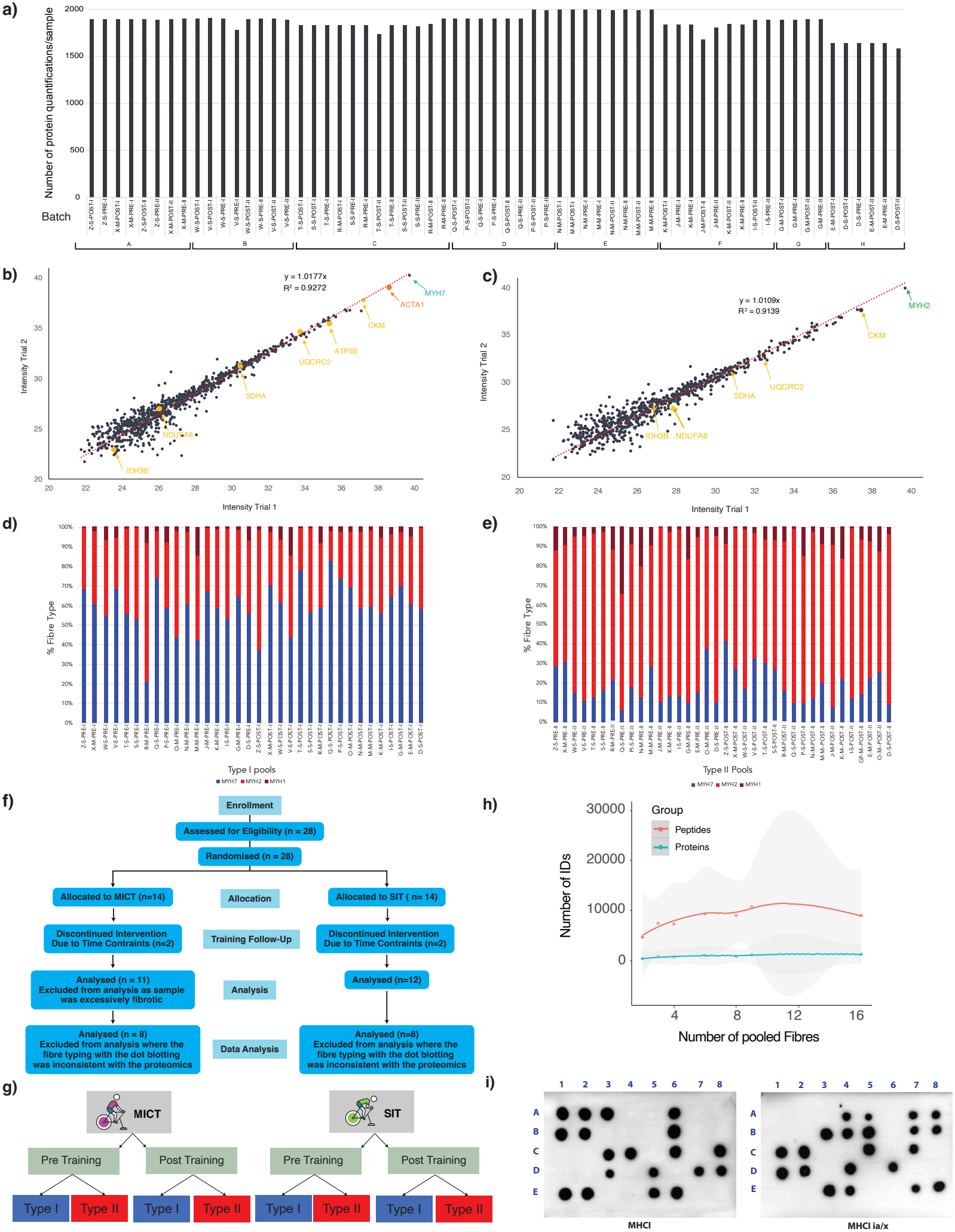
a)
Number of protein quantifications/sample
Batch
b)
y = 1.0177x
R² = 0.9272
MYH7
ACTA1
CKM
ATP5B
UQCRC2
SDHA
NDUFA8
IDH3B
Intensity Trial 1
Intensity Trial 2
c)
y = 1.0109x
R² = 0.9139
MYH2
CKM
UQCRC2
SDHA
IDH3B
NDUFA8
Intensity Trial 1
Intensity Trial 2
d)
% Fibre Type
Type I pools
MYH7 MYH2 MYH1
e)
% Fibre Type
Type II Pools
MYH7 MYH2 MYH1
f)
Enrollment
Assessed for Eligibility (n = 28)
Randomised (n = 28)
Allocated to MICT (n=14)
Allocation
Allocated to SIT (n= 14)
Discontinued Intervention Due to Time Contraints (n=2)
Training Follow-Up
Discontinued Intervention Due to Time Contraints (n=2)
Analysed (n = 11) Excluded from analysis as sample was excessively fibrotic
Analysis
Analysed (n=12)
Analysed (n = 8) Excluded from analysis where the fibre typing with the dot blotting was inconsistent with the proteomics
Data Analysis
Analysed (n=8) Excluded from analysis where the fibre typing with the dot blotting was inconsistent with the proteomics
h)
Group
Peptides
Proteins
Number of IDs
Number of pooled Fibres
g)
MICT
SIT
Pre Training
Post Training
Pre Training
Post Training
Type I
Type II
Type I
Type II
Type I
Type II
Type I
Type II
i)
MHCI
MHCI ia/x

Supp Fig.2